IEEE Open Journal of
Power Electronics

Received 15 September 2022; revised 18 October 2022; accepted 23 October 2022. Date of publication 27 October 2022; date of current version 10 November 2022. The review of this article was arranged by Associate Editor Giampaolo Buticchi.

Digital Object Identifier 10.1109/OJPEL.2022.3217741

Grid Integration of DC Buildings: Standards, Requirements and Power Converter Topologies

EDIVAN LAERCIO CARVALHO [1] (Member, IEEE), ANDREI BLINOV [1] (Senior Member, IEEE), ANDRII CHUB [1] (Senior Member, IEEE), PIETRO EMILIANI [1] (Student Member, IEEE), GIOVANNI DE CARNE [2] (Senior Member, IEEE), AND DMITRI VINNIKOV [1] (Senior Member, IEEE)

[1]Department of Electrical Power Engineering and Mechatronics, Tallinn University of Technology (TalTech), Ehitajate Tee 5 19086 Tallinn, Estonia
[2]Institute for Technical Physics, Karlsruhe Institute of Technology, 76227 Eggenstein-Leopoldshafen, Germany

CORRESPONDING AUTHOR: EDIVAN LAERCIO CARVALHO (e-mail: edivan.carvalho@taltech.ee)

This work was supported in part by the Estonian Research Council under Grant PRG1086 and in part by the Estonian Centre of Excellence in Zero Energy and Resource Efficient Smart Buildings and Districts under Grant 2014-2020.4.01.15-0016, funded by the European Regional Development Fund. The work of Giovanni De Carne was supported in part by Helmholtz Association through the Program Energy System Design and in part by the Helmholtz Young Investigator Group Hybrid Networks under Grant VH-NG-1613.

ABSTRACT Residential dc microgrids and nanogrids are the emerging technology that is aimed to promote the transition to energy-efficient buildings and provide simple, highly flexible integration of renewables, storages, and loads. At the same time, the mass acceptance of dc buildings is slowed down by the relative immaturity of the dc technology, lack of standardization and general awareness about its potential. Additional efforts from multiple directions are necessary to promote this technology and increase its market attractiveness. In the near-term, it is highly likely that the dc buildings will be connected to the conventional ac distribution grid by a front-end ac-dc converter that provides all the necessary protection and desired functionality. At the same time, the corresponding requirements for this converter have not been yet consolidated. To address this, present paper focuses on various aspects of the integration of dc buildings and includes analysis of related standards, directives, operational and compatibility requirements as well as classification of voltage levels. In addition, power converter configurations and modulation methods are analyzed and compared. A classification of topologies that can provide the required functionality for the application is proposed. Finally, future trends and remaining challenges pointed out to motivate new contributions to this topic.

INDEX TERMS Ac-dc power conversion, energy-efficient buildings, dc distribution systems, microgrids, standardization.

NOMENCLATURE

1F	Single-phase.
3F	Three-phase.
2L	Two-level.
3L	Three-level.
ANPC	Active neutral point clamped.
CF-DAB	Current-fed dual-active bridge.
DAB	Dual-active bridge.
DERs	Distributed energy resources.
DPSM	Dual phase-shift modulation.
EEMS	Electrical energy management system.
ELVDC	Extra-low voltage direct current.
EPSM	Extended phase-shift modulation.
EV	Electrical vehicles.
FM	Frequency modulation.
i-AFE	Isolated active front-end.
LVD	Low voltage directive.
LVDC	Low voltage direct current.
NPC	Neutral point clamped.
nZEB	Net-zero energy building.
OVRT	Overvoltage ride-through.
PEIs	Prosumer electrical installations.

PELV	Protective extra low-voltage.
PFC	Power factor correction.
PSM	Phase-shift modulation.
PSUs	Power supply units.
PV	Photovoltaic.
PWM	Pulse width modulation.
q-SS	Quasi-single-stage.
SELV	Separated extra low voltage.
SPSM	Single phase-shift modulation.
SS	Single-stage.
SST	Solid-state transformer.
TPSM	Triple phase-shift modulation.
TS	Two-stage.
UPS	Uninterruptible power supply.
UVRT	Undervoltage ride-through.
VC	Voltage control.
VR	Voltage regulation.
VSC	Voltage source converter.
ZVS	Zero voltage switching.

I. INTRODUCTION

The development of new standards for prosumer dc electrical installations, such as the IEC 60364 series and NPR 9090, has put spotlight on the dc microgrids and nanogrids [1], [2], [3]. These developments are motivated by the advances in power electronics and the growing interest to develop green, smart, and highly efficient power distribution systems [4], [5], [6], [7], [8], [9]. Prosumer electrical installations (PEIs) [7] are applied in homes, offices, and other buildings, where dc distribution is attractive because renewable power sources and many loads operate at dc, but have to be adapted to ac using ac-dc converters [2], [8], [9], [10], [11], [12].

For instance, dc loads require a three-phase PFC rectifier to supply a dc bus from the ac utility grid [8], [9]. In addition, galvanic isolation can be obligatory due to grounding schemes and safety requirements [3], [9]. These ac-dc converters increase the number of power processing stages, reducing the overall system efficiency [3], [4], [5]. In addition, they are required to provide synchronization, power factor correction (PFC), active and reactive power control, as well as other services related to ac systems [12], [13], [14].

Considering these reasons, dc distribution could be a key solution for future PEIs [4], [5]. Many recent projects have been initiated to develop near-zero and net-zero energy buildings (nZEBs) based on dc distribution [2]. The findings have shown that it saves costs, improves the system reliability, and increases the power density of PEIs [6], [15], [16], [17]. Even though the dc integration of power generation and loads is still an underdeveloped topic, in the last few years, significant steps have been made in the development of power electronics solutions and standardization [2].

Main efforts to standardize dc distribution systems are demonstrated in the directive LVD (2014/35/EU) [18], IEC 6034 series [19], [20], [21], [22], [23], [24], [25], and NPR 9090 [26]. These standards cover a range of aspects, from power electronic devices to safety requirements [6], [19], [20], [21], [22], [23], [24], [25]. NPR 9090 was the first national practice guideline for residential LVDC systems, defining the protection zones and the isolation requirements [1], [26]. Fig. 1 shows the main safety zones and the risks classification interpreted from NPR 9090 in [1]. A critical requirement of the NPR 9090 is the galvanic isolation between the ac and dc sides [26]. Even though no specific standard is available for ac-dc active front-end converters, new developments target mostly isolated converters.

Two-stage (TS) isolated ac-dc converters [see Fig. 2(a)] are presently the standard solution in industrial applications. In the two-stage system, an ac-dc active front-end converter is used to control the power factor on the ac side and to regulate the intermediate dc bus voltage. On the dc side, a dc-dc stage provides high-frequency isolation [27], [28], [29], [30], [31], [32]. The use of two-stage solutions has some advantages, including the capability to handle high power levels [33], [34], [35]. On the other hand, all input power is processed twice [35], [36], adding sensors and control loops to implement the control of two stages [37]. Quasi-single-stage (q-SS) converters feature no decoupling dc-bus capacitor [see Fig. 2(b)]. This allows an increase in the converter power density and saves costs in some applications because the decoupling capacitors are usually bulky [38].

Additionally, several papers have proposed single-stage (SS) converters to replace two-stage and q-SS solutions. Therefore, a series of new topologies, which integrate the PFC (ac-dc conversion) and isolation in the same stage, has been proposed [39], replacing single semiconductors with anti-series switches [see Fig. 2(c)]. This reduces the number of power processing stages and control requirements because only the input current (i_{ac}), and the output voltage (v_{dc}) need to be controlled [37], [38], [39]. The potential benefits of q-SS and single-stage converters significantly increase the number of possible isolated ac-dc converter topologies, including matrix-based DAB [39], [40], [41], [42], [42], [44], [45], T-type based [46], [47], [48], [49], [50], interleaved converters [51].

Emerging topologies such as single-stage have not yet reached maturity and good industrial awareness. There is still lack of practical experience regarding evaluation of the feasibility of different solutions for specific applications. In addition, no specific standards are available for active front-end converters in residential dc systems. As result, it is challenging to define design requirements and fair criteria to compare different solutions.

To address this knowledge gap, this paper reviews the topologies, design requirements, and functionalities for isolated active front-end (i-AFE) converters. The review highlights further developments in the overviewing single-stage i-AFE solutions [38]. A classification of topologies is presented, and current standards are discussed to prospect future directives for i-AFE converters. The objective is to present the latest developments of i-AFE for the ac grid and dc building

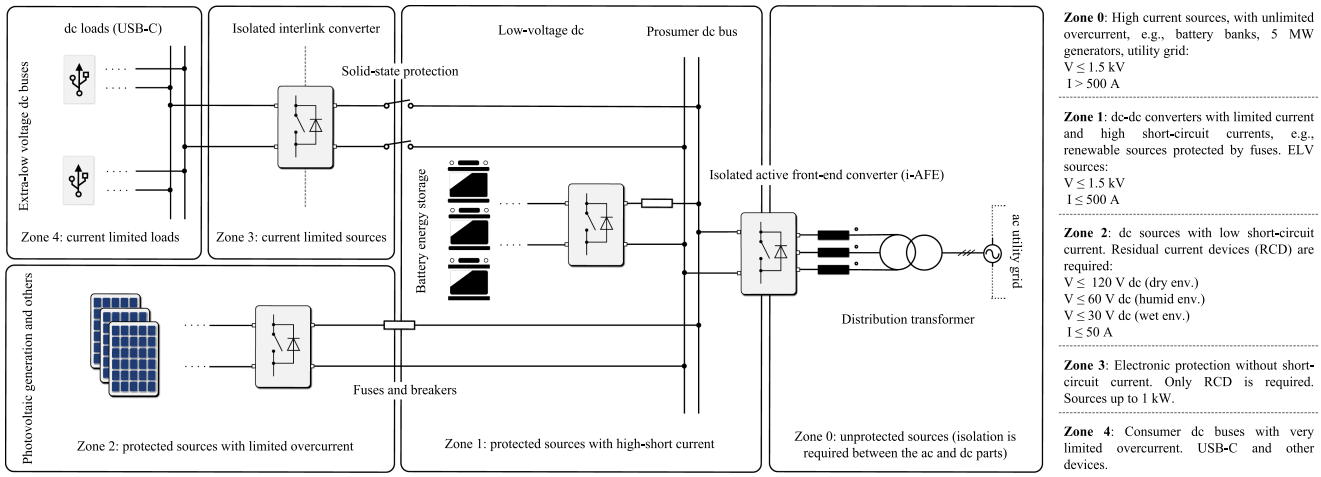

FIGURE 1. **Interpretation of safety zones in the dc distribution system according to NPR 9090 [1].**

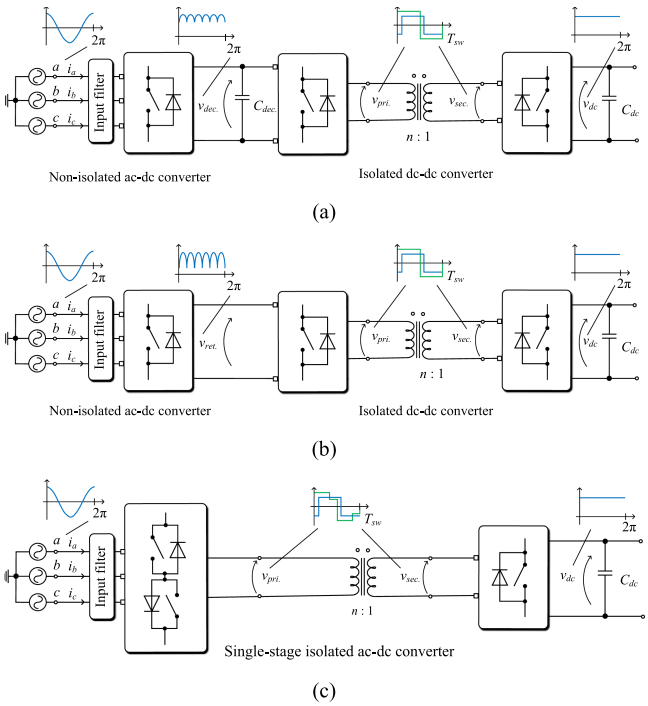

FIGURE 2. **i-AFE converter solutions: (a) a two-stage (TS) isolated ac-dc converter; (b) no intermediate dc bus required in a quasi-single-stage (q-SS) converter; (c) fully controlled switches used to integrate the PFC stage in the isolated converter for single-stage (SS) converters [39].**

integration, highlighting open problems and opportunities for new research. Considering all these aspects, the main contributions of this paper are the following:

1) Review of current standards and directives for dc electrical installations and correlated power electronic devices. This discussion is essential to define the main design requirements for i-AFE converters in dc buildings. In addition, this is important for prospective specific standards for i-AFE converters. The support of standards is mandatory for new solutions that must perform adequately in real systems.
2) Overview of dc loads and standard voltage levels for dc electrical installations, which helps to define the main design parameters for i-AFE converters. In addition, this is essential for contextualizing their application.
3) Proposal of classification for dc bus voltages. The classification is based on an overview of dc loads and current-voltage levels used in dc systems projects. This helps not only to define design parameters for i-AFE converters but can also be used as design guidelines for dc electrical installations.
4) A classification of i-AFE converter topologies. This analysis presents the topologies that could enhance the benefits of dc systems. In addition, this enables unbiased comparison of different solutions.

This paper is organized as follows: Section II discusses the design requirements for i-AFE converters according to the standardization and directives for dc systems and provides a classification of dc bus voltage levels according to their applications. Section III introduces a classification for i-AFE converters, presenting an overview of different i-AFE topologies. Current developments and their applications are presented. Section IV presents a summary and discusses future trends and challenges for i-AFE converters. In addition, suggestions for future works are proposed. Section V presents general conclusions of this study.

II. OPERATIONAL REQUIREMENTS AND STANDARDIZATION FOR FUTURE ISOLATED ACTIVE FRONT-END CONVERTERS

To distinguish the most feasible power electronics solutions for i-AFE converters, it is required to discuss the standardization of dc microgrids and electronic devices for distributed energy resources (DERs). This study evaluates different converter topologies and defines their functionalities and design requirements. Even though no specific standards are ready for

i-AFE converters, new directives and standardization should be investigated for further developments. Therefore, this section focuses on the analysis of current standards and works in correlated areas.

Table 1 lists the current standards and possible applications that may be related to i-AFE converters. The main requirements are brought out since they could be used as a reference and guideline for future i-AFE developments. These requirements are divided according to their applicability between: *i*) protection and safety requirements; *ii*) compatibility with dc microgrids; *iii*) compatibility with ac grid and power quality; *iv*) functionalities, such as power management and communication.

A. PROTECTION AND SAFETY REQUIREMENTS FOR AFE CONVERTERS

The main requirements for protection are related to end-user safety. However, internal protections are also important to avoid explosions and fire risks. The following requirements related to equipment protection are highlighted:

i) *Overvoltage protection*: IEC 62109-1, IEC 62109-2
ii) *Short-circuit and overload protection*: IEC 62109-1, IEC 62109-2
iii) *Protection against internal failures and bad connections*: IEC 62109-1 and IEC 62109-2.

Two additional requirements related to user safety should also be mentioned [26]:

i) *Protection against electric shock: LVD (2014/35/EU), IEC 62040-1*
ii) *Overtemperature, fire safety, and other cases: LVD (2014/35/EU), IEC 62040-1.*

In addition, i-AFE converters must meet requirements for dc electrical installations. The NPR 9090 divides dc installations into four protection zones according to the voltage and current levels:

Zone 0: unprotected sources, where very high overcurrent is possible (1 kV $< v_{dc} <$ 1.5 kV, $i_{dc} >$ 500 A), including PV and energy storage at utility scale
Zone 1: protected sources with high short-circuit current, where it is possible to include passive protection.
Zone 2: protected sources with limited overcurrent and multiple sources
Zone 3: prosumer dc buses with very limited overcurrent; could be installed inside buildings
Zone 4: ELVDC dc buses without significant overcurrent; in this zone, there are only users of electrical energy.

According to the protection zones and requirements of NPR 9090, the ac and dc parts of dc microgrids must be isolated. The main motivation to provide galvanic isolation between the ac grid and the dc microgrid is related to the grounding system. With isolated i-AFE converters, it is possible to provide TNS-type groundings, which simplifies the electronic protection, reduces common-mode voltage, and increases the safety of the end-users [65]. The grounding and other requirements for safety are standardized by the IEC 60364-4-41 and IEC 60479. In addition, IEC 60364-5-53 and IEC 60364-7-710 can be applied in a complementary way to cover critical installations, such as hospitals, surgery rooms, and other units.

B. REQUIREMENTS FOR THE COMPATIBILITY WITH DC MICROGRIDS

The requirements to meet the i-AFE converter design with dc microgrids are related to the dc bus capacitance dimensioning, electromagnetic compatibility, voltage ripple, and holdup time:

i) *EMC requirements:* according to IEC 62040-2, IEC 61000-6-3, and IEC 61000-6-4.
ii) *Compatibility with dc loads:* necessary to meet the holdup time, voltage ripple, and voltage regulation range, according to IEC 61000-4-11 and IEC 62040-5-3.
iii) *Holdup time:* time interval when the output voltage stays within pre-defined limits in the case the input power is lost. IEC 61000-4-11 provides the minimum holdup time of 10 *m*s (one half-cycle of 50 Hz line frequency).

C. COMPATIBILITY WITH AC GRID AND POWER QUALITY

The AFE converters must operate synchronized with the ac grid, handling a sinusoidal current. It is important to ensure high power-factor and high power-quality at the point of common coupling in either rectifier or inverter operation modes. In addition, it is essential to provide basic functions to ensure support to the grid when necessary. The main requirements for the ac side are defined by IEC 61000-3-15 [61] and IEC TS 62786 [64], including:

i) *Total harmonic distortion (THD):* defined by IEC 61000-3-15
ii) *Individual harmonics requirements:* where the harmonic limits are defined by IEC 61000-3-15
iii) *DC current injection:* not allowed by the IEC 61000-3-15
iv) *Power factor:* defines the minimum power factor considering the AFE converter operation in a normal condition (without active/reactive power control). The power factor can be reduced to assist the grid stability under voltage variations conditions – when required by external command [64].
v) *Voltage fluctuations:* range of voltage variation near the nominal condition, where it is possible to maintain the i-AFE converter connected to the grid
vi) *Flicker*: defines the limits of flicker emission
vii) *Active and reactive power control:* to reduce the active power to assist the grid stability during frequency variations
viii) *Overvoltage and undervoltage ride-through:* the i-AFE converters must withstand instantaneous voltage variations of the ac grid. The voltage limits and time to disconnect under OVRT and UVRT are provided in IEC TS 62786 and IEC TR 61850-90-7.

TABLE 1. Related Standards and Their Possible Application in AFE Converters

Standard reference	Scopes	Application	Directives for AFE converters design
IEC 62109-1 [52] IEC 62109-2 [53]	Safety requirements of power electronics converters, including protection against simple failures	PV converters, including stand-alone and hybrid systems	Safety requirements and protection, during failures in AFE converter components
IEC 62040-1 [54]	Safety requirements for UPSs installed in accessible areas	UPSs at low voltage ac, not exceeding 1000 V ac or 1500 V dc	Safety requirements for AFE, which can be installed inside of a house or office.
NPR 9090:2018 [26]	DC installations for low voltage (up to 1500 V dc). Defines the safety areas of dc microgrids according to the voltage levels.	Dc microgrids at the distribution level (between 350 V and 1500 V dc)	Necessary to match the AFE converter design with dc microgrids requirements. Galvanic isolation must be applied between the ac and dc parts.
LVD (2014/35/EU) [18]	Directive for low voltage dc equipment (between 75 V and 1500 V dc)	Electrical equipment, such as home appliances, power supply units, lases, fuses, and others	Requirements for the user protection against electrical shocks
IEC 60364-4-41 [20] IEC 60479 [55]	Protection against electric shock, protection devices for safety and isolation requirements	Low voltage electrical installations at small buildings	Complementary to the NPR 9090 and LVD (2014/35/EU), including classification and grounding requirements
IEC 60364-5-53 [21] IEC 60364-7-710 [22]	Safety for electrical installations in medical locations	Electrical installations in clinics, hospitals, and equivalents (homes for senior citizens, etc.)	Safety requirements in critical electrical installations, such as hospitals and similar
IEC 62040-2 [56]	Electromagnetic compatibility (EMC) requirements	UPSs at low voltage ac, not exceeding 1000 V ac or 1500 V dc	Compatibility of AFE converter with loads in distribution systems (residential, commercial, or industrial)
IEC 61000-4-11 [57]	Voltage dips, short interruptions, and voltage variations immunity tests	Generation systems up to 75 A_{rms} per phase (power converters connected to low voltage networks)	Defines the voltage variation and holdup time, required to design dc bus capacitances
IEC 61000-6-3 [58] IEC 61000-6-4 [59]	Emission requirements applied to electrical and electronic equipment	Equipment for residential and industrial environments	EMC requirements for PCBs and EMC filters design
IEC 62040-5-3 [60]	Tests requirements and performance of UPSs to supply dc loads.	UPSs at low voltage ac, not exceeding 1000 V ac or 1500 V dc	Defines requirements for AFE converters to supply dc loads
IEC 61000-3-15 [61]	Limits of EMC, and power quality	Generation systems up to 75 A_{rms} per phase (power converters connected to low voltage networks)	Defines limits and tests for ac current harmonics, voltage fluctuation, flicker, dc current injection, and others
IEC 62116 [62]	Test procedures of islanding prevention for grid-connected PV inverters	Grid-connected PV inverters	Anti-island protection, requirements, and test procedures
IEC 60364-8-1 [23] IEC 60364-8-2 [24] IEC 60364-8-3 [25]	Additional requirements, including the power management for low voltage prosumer electrical installations	Low voltage prosumer electrical installations (PEIs)	Meets the AFE functionalities with the power management requirements, including droop control, or similar, when necessary to ensure the power balance at dc side
IEC TR 61850-90-7 [63]	Describe the main functions of power converters in distributed energy resources (DERs) systems	PV converters, battery energy storage systems, EVs, and others	Defines the main functionalities of AFE converters to allow managing the volt, var, and watt capabilities
IEC TS 62786 [64]	Specifications and requirements for distributed energy resources connected to the distribution network	Distribution generation connected to the distribution network, including generating plants at medium and low voltage ac	General capabilities of AFE converter as smart inverter: • Anti-islanding protection • Under / Overvoltage ride-through (UVRT and OVRT) • Dynamic Volt/Var operation • Ramp rates • Power factor control • Monitoring, communication, energy management, and others.

ix) *Disconnection in abnormal voltage conditions:* the AFE converter must be disconnected under abnormal voltage conditions in a time less than the limits defined by the IEC TS 62786.
x) *Anti-islanding protection:* it is necessary to identify and avoid unintentional islanding operations, following the criteria of IEC 62116, IEC 61000-3-15 and IEC TS 62786.
xi) *Reconnection requirements:* defines the reconnection time according to the requirement of IEC 61000-3-15 and IEC TS 62786

Regarding the functionalities and control methods for ac-dc converters under voltage variations, in [66] and [67], possible solutions, including OVRT and UVRT operation and anti-island protection, are presented. As for voltage variations, the current standards mainly cover converter operation as an inverter, for example, in PV systems. On the other hand, the i-AFE converters also operate as a rectifier, which should be considered in future directives.

D. ADDITIONAL REQUIREMENTS

Besides the requirements addressed in the previous sections, it is necessary to allow the i-AFE converters to operate with external commands to optimize energy management. The additional features related to power management rely on networks and communication protocols. Commonly used communication protocols for power converters include DNP3 or Modbus [68]. Even though the communication systems are out of the paper's scope, the IEC TR 61850-90-7 describes the communication networks, security requirements, and the additional functions for power converters. For that reason, it can be used as a complementary reference. The main features covered by IEC TR 61850-90-7 include:

i) *Communication networks:* communication links and compatible protocols are required to allow the AFE converter to respond to external control signals.
ii) *Ramp rates:* standard rates of ac current to allow soft-connection or reconnection.
iii) *Temperature derating:* power processing reduction to avoid undesirable internal temperatures.
iv) *Volt and VAR control:* possible to be controlled according to external signals.
v) *Power factor management:* possible to be controlled according to external signals.
vi) *Request active power:* necessary to ensure the power balance according to the energy management system.
vii) *Energy management:* previewed in the IEC 60364-8 to ensure the system's smart operation.

These capabilities can be used to exchange information between i-AFE converters and the electrical energy management system (EEMS). The IEC 60364-8 series provide the main requirements to manage prosumer electrical installations [6], [66]. This is necessary to provide power balance and save energy in nZEB.

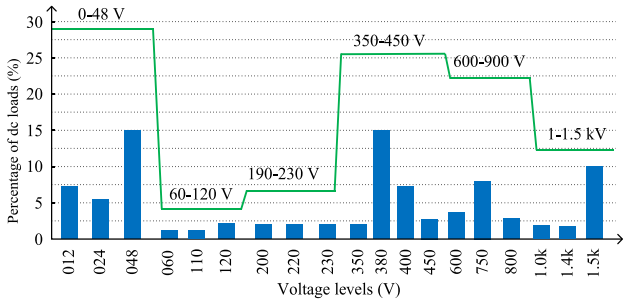

FIGURE 3. Common dc bus voltage in existing applications [14].

E. CLASSIFICATION OF DC BUS VOLTAGES AND PROTECTION ZONES

In addition to the standards, operational, and safety requirements, the voltage levels for dc microgrid/nanogrids are another important topic to be discussed. The compatible voltage levels are required for matching the i-AFE converter design with current standards for dc loads. Related to the ac side, nominal voltages of 110-240 V_{rms} for single-phase and 380-400 V_{rms} for three-phase systems are common. On the other hand, for dc loads, the supply voltage levels range from extra-low voltages (ELVDC) to hundreds of volts at LVDC.

The IEC report [14] presents an overview to identify the main rated voltages used in dc applications [see Fig. 3]. A high number of dc loads are found in homes and offices, such as LED lighting, computers, and home appliances. In these applications, it is mandatory to ensure safety against electric shocks, which makes the adoption of ELVDC levels interesting. In addition, some industrial systems are also based on ELVDC to simplify service and maintenance. For example, in telecommunication, many critical dc loads are supplied with 12 V, 24 V, or 48 V.

On the other hand, extra-low voltage buses are naturally limited in terms of power processing and distances since high currents and long distances result in high power losses. According to the reference [14], ELVDC buses must be applied only at short distances and at low power levels (less than 1 kW).

LVDC levels between 350 and 450 V are commonly used in data centers, racks, servers, and other industrial applications. For example, 380 V dc is a common voltage in power supply units (PSUs) and UPSs [9], [14], [69], [70]. These LVDC levels allow an increase in the power processed inside homes, offices, and light industrial installations (such as nanogrids) [6], [26].

For the highest voltage level bands (600-900 V and 1-1.5 kV), the main difficulty is related to the safety and protection requirements. Therefore, these voltage ranges are not typical for residential-scale microgrids [26], where end-user could be harmed.

To define the possible voltage ranges at the dc side, the IEC report [14] and project report [65] were analyzed. A classification for dc buses is proposed in Table 2. It can be used

TABLE 2. Proposed Classification of the Main DC Buses for DC Microgrids

Voltage level	Safety and protection	Standardization	dc bus classification	Power levels	Application
0-48 V dc	Non-protected SELV and PELV, including bipolar systems	IEC 60364	ELVDC auxiliary dc buses (Zone 4)	Up to 1 kW, according to the IEC report [13]	Electronic devices with limited output current, including home appliances, TV sets, and lighting. Critical loads at data centers, medical equipment, emergency lighting, and others.
60-120 V dc	Non-protected only in 3-wire systems	IEC 60364	Auxiliary dc buses (Zones 3, 2 or 1 according to the protection requirements)	Less than 6 kW [13]	Typical household and office load, higher than 1 kW. Can be applied in dc microgrids in remote areas as well in residential and commercial buildings
190-230 V dc	Fuse protected				
350-450 V dc	Semiconductors and fuse protection	IEC 60364 NPR 9090	Main dc bus for building-scale microgrids (nanogrids) (Zone 1)	Up to 20 kW [65]	Distribution dc bus inside of homes, offices, hospitals, and other prosumer electrical installations (PEIs).
600-900 V dc	High risk *	IEC 60364 NPR 9090	Main dc bus for industry-scale microgrids (Zone 1)	Less than 0.5 MW [65]	Industry, transportation, and other highest power applications, less than 0.5 MW.
1-1.5 kV dc	High risk *	IEC 60364 NPR 9090	Utility-scale dc bus (Zone 0)	Higher than 0.5 MW [65]	Utility-scale PV plants and microgrids at the power distribution level.

*Could kill in case of direct contact, according to the IEC 60479.

as a design guideline for further work. The safety zones are indicated for each dc bus according to their voltage levels and functionalities, following NPR9090 [see Fig. 4]. In addition, reference [65] indicates acceptable voltage deviations for the main dc buses for industry and building-scale microgrids [see Fig. 5].

The voltage deviations must be defined to avoid unintended disconnections during transients. Voltage deviations could occur according to the power management strategy based on droop control with dc-bus signaling [6].

Reference [6] compares different power management methods in terms of dc bus voltage deviations. For centralized controllers, the dc voltage deviation can be reduced by applying a proper communication link. However, for decentralized controllers, such as droop-based, the deviation increases and must be handled by the i-AFE converter. In this way, [65] can be used as a design guideline for the droop-based controllers.

F. GENERAL REMARKS ON THE CURRENT STANDARDS AND REQUIREMENTS FOR I-AFE CONVERTERS

The standardization of dc microgrids, ac grids, and electronic devices is important to define the main requirements for the AFE converters. The main goal of this section was to analyze and prospect these requirements.

Even though no specific standards are ready for i-AFE converters, analysis of the existing standards gives guidance to the research of power converter topologies and the most feasible future solutions can be identified. The following section focuses on the analysis and characterization of different power converters, which could be candidates to cope with the main requirements for i-AFE converters, including bidirectional operation capability, control over the power factor, high-frequency isolation, required voltage regulation range, and other parameters.

III. ISOLATED AC-DC POWER CONVERSION: OVERVIEW OF TOPOLOGIES AND CLASSIFICATION

Conventional ac-dc converters are intended to act as rectifiers with a unity power factor. For example, boost-type converters that follow the passive diode bridge rectifiers are used for the power factor correction for lighting loads [66], [67], [68], [69], [70], [71], [72], home appliances [73], [74], and other devices [75], [76]. However, additional features are necessary in dc microgrids, as was discussed in Section II. i-AFE converters for dc microgrids and nanogrids need to go beyond basic functions, providing grid support through voltage and frequency regulation, active and reactive power control, and being able to handle bidirectional power flow – due to the insertion of renewables at the user side (prosumer dc buses) [26], [77], [78]. These functionalities allow i-AFE converters to act as smart (multifunctional) inverters providing support for the ac grid, while continuously managing the dc microgrid [79].

A few different topologies can be capable of meeting these requirements. In addition, different power converters can be connected when more than one power processing stage is used. This results in many possible topology configurations, whereas no classification and benchmarking was found for i-AFE converters in the existing literature. In this paper is proposed the following classification for i-AFE converter topologies:

i) Firstly, each group of topologies must be divided according to their power processing stages, namely two-stage (TS), quasi-single-stage (q-SS), and single-stage (SS) topologies [see Fig. 2].
ii) i-AFE converters can be divided according to the number of voltage levels at the ac side, e.g., two-level (2L) or multilevel (e.g., three-level (3L) topologies).
iii) Finally, the i-AFE converters are divided according to the topology at the dc side, where several classes of

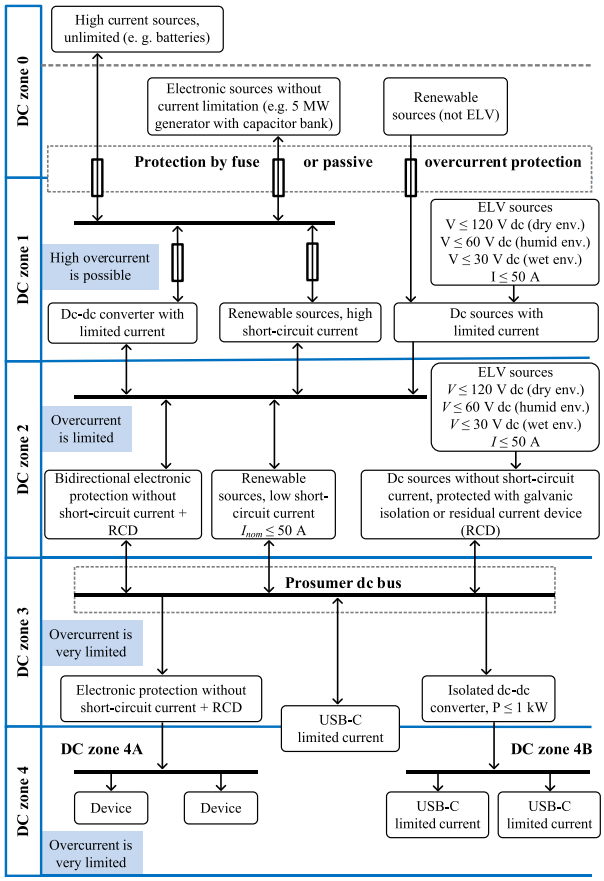

FIGURE 4. Safety zones and protection requirements for dc distribution according to NPR 9090 [26].

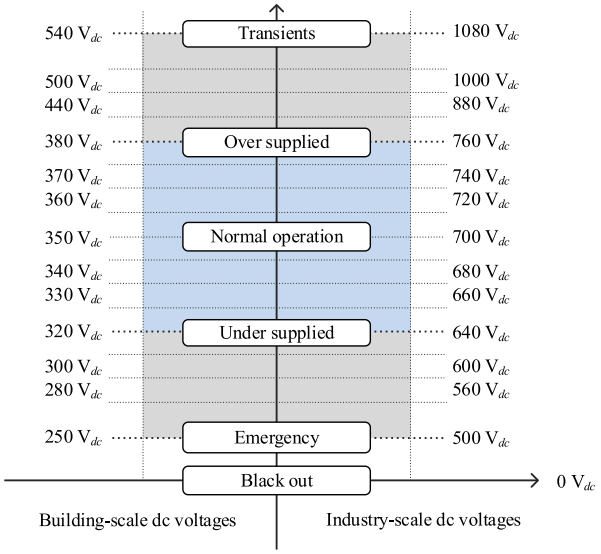

FIGURE 5. Voltage levels and limits for LVDC electrical installations [65].

power converters can be found. This division must be in accordance with the number of power processing stages and modulation strategy.

It should be noted that criteria (*ii*) and (*iii*) are independent once the ac-dc and dc-dc stages can be separated. In this sense, there are no hierarchical levels between the ac and the dc side to classify the i-AFE converters. In this paper, the ac side was chosen to start the classification arbitrarily. The main classes of i-AFE converter topologies are presented in Fig. 6. From this classification, each group of i-AFE converters is revised in the following subsections according to their power processing stages.

A. TWO-STAGE I-AFE CONVERTERS: AC-DC TOPOLOGIES

Considering the requirements previously described, several topologies can be applied to the PFC stage. In telecommunication systems, for example, the totem-pole PFC is the most widespread solution [79], [80], [81]. The totem-pole rectifiers are connected with the dual-active bridge converter for battery chargers and PSUs up to 6 kW [70]. On the other hand, this kind of solution cannot be directly applied to three-phase systems, which limits its application to i-AFE converters.

For the three-phase systems, the leading industrial solutions generally narrow down the two-level voltage source converter (2L-VSC) and the multilevel topologies, where the three-level neutral point clamped (3L-NPC) is the most used topology. Despite many other topologies proposed and tested as ac-dc converters, the two abovementioned alternatives are typically employed in the industry due to their maturity, cost-effectiveness, efficiency, and reliability [1]. In addition, the T-type NPC was gaining attention in the last years due to the new developments of integrated power modules. These alternatives will be analyzed in detail in the following sections.

1) TWO-LEVEL VOLTAGE SOURCE CONVERTER (2L-VSC)

The two-level voltage source converters (2L-VSC) are found in many industrial applications for ac-dc power conversion. Their common usage includes drives for electric motors, UPSs, battery chargers, and power factor correction for electronic devices [69], [82], [83], [84], [85]. The power circuit in Fig. 7 includes six semiconductor devices and a dc bus on the dc side. For four-wire systems, an extra leg (S_7-S_8) can be used. On the ac side, first-order (*L*) and third-order (*LCL*) filters can be options for the ac grid connection. The ac filters must be designed to avoid high-frequency harmonics and to shape a sinusoidal current.

As for the semiconductor technology used, the MOSFETs or IGBTs are the typical options depending on the power level being processed and the switching frequency. In terms of power-module developments, many semiconductor manufacturers offer integrated solutions between 600 V and 1200 V. Additionally, silicon carbide (SiC) MOSFETs have been widely adopted in recent years, including either integrated or discrete devices [86], [87].

One advantage in this topology is that it is possible to ensure zero-voltage switching (ZVS) if an appropriate dead-time is introduced between series semiconductors [35], [69]. The conduction of series semiconductors is prohibited, which is a restriction of this topology.

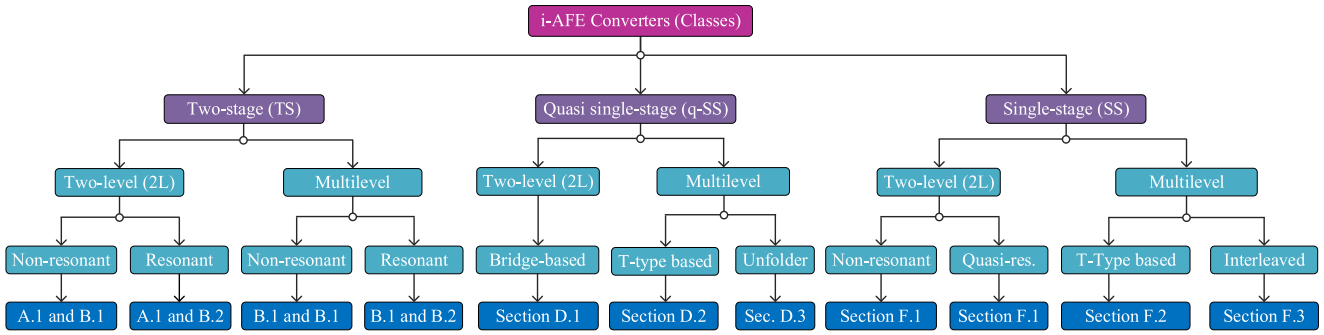

FIGURE 6. General classification of i-AFE converters according to the power processing stages and possible topologies for ac and dc sides.

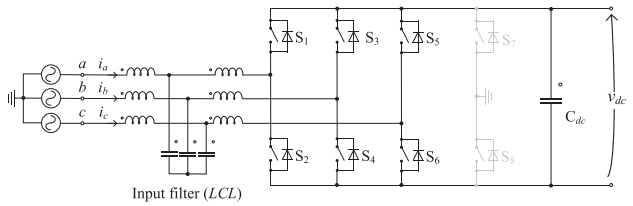

FIGURE 7. Three-phase 2L-VSC PFC. Three-legs are used to connect to the ac grid with three-wire systems. In four-wire systems, an additional leg (S_7-S_8) is necessary to connect to the neutral point. For the ac side, *LCL* and *L* filters are possible.

However, several modulation strategies are possible, including carrier-based and space-vector modulations [88]. For i-AFE converters, the 2L-VSC is commonly connected with the dual-active bridge or resonant topologies at the dc side [69]. Current developments for two-stage solutions range from 3 kW to 20 kW at LVDC. Additionally, many single-stage and quasi-single-stage topologies are derived from the 2L-VSC.

2) THREE-LEVEL NPC (3L-NPC)

Although other multilevel topologies could be implemented in the PFC stage, the three-level neutral point clamped (3L-NPC) is the most widespread topology in industrial applications. The main motivations for the NPC adoption include low harmonics compared to two-level 2L-VSC and high reliability because the NPC is based on a diode clamp, which is an advantage over other three-level converters based on flying capacitors [79], [87], [88].

The conventional 3L-NPC is presented in Fig. 8(a), including four active semiconductors and two clamping diodes for each phase. The clamping diodes are connected to the neutral point of the dc bus. The shared dc bus allows for reducing the voltage stress of semiconductors, increasing efficiency and power processing rates [89].

Regarding semiconductor technology, IGBTs and MOSFETs could be employed. However, one disadvantage of this topology is in the *rms* current of the clamping diodes. During non-unity power factor operation, the diode current increases power losses, and the NPC efficiency is reduced

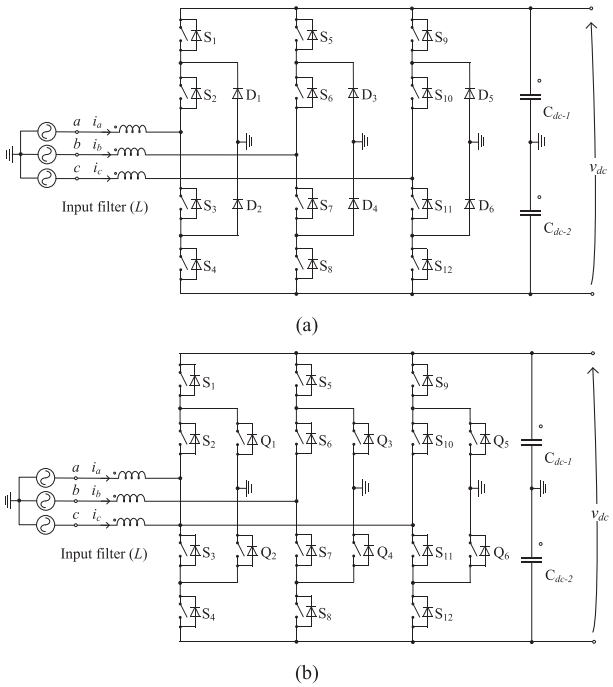

FIGURE 8. Neutral-point-clamped ac-dc converters: (a) the conventional NPC converter, where the clamping diodes could be replaced with active semiconductors in the ANPC converter; (b) the active neutral point clamped (ANPC) converter.

[87]. Therefore, some manufacturers have been developing power-modules with only active semiconductors.

The active neutral point clamped (ANPC) topology is presented in Fig. 8(b). ANPC allows optimization of the power-modules with the combination of different semicon ductor technologies, for example, Si-SiC, Si-IGBT, and Si-SiC-IGBT [87]. Reference [87] compares different arrangements of semiconductors in APNC topology in terms of losses, price, and design requirements. These criteria must be analyzed according to the application and power processed levels.

3) T-TYPE NPC

Even though the T-type topology is not very common in a two-stage i-AFE, it is important to introduce the topology

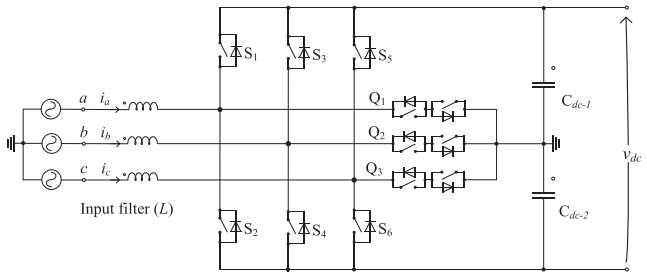

FIGURE 9. T-type NPC converter. The fully controlled switches Q_1, Q_2, and Q_3 are implemented with anti-series semiconductors. It is necessary to clamp the neutral point, replacing the clamping diodes of the conventional NPC.

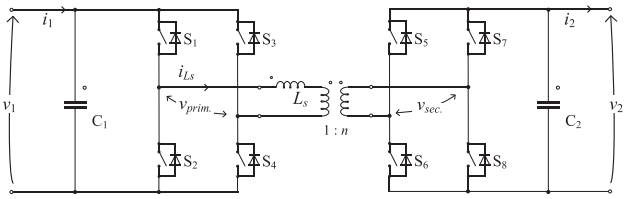

FIGURE 10. Dual-active bridge converter, where the leakage inductance (L_s) is used as an energy storage element, and two active bridges are used to control the power flow between v_1 and v_2.

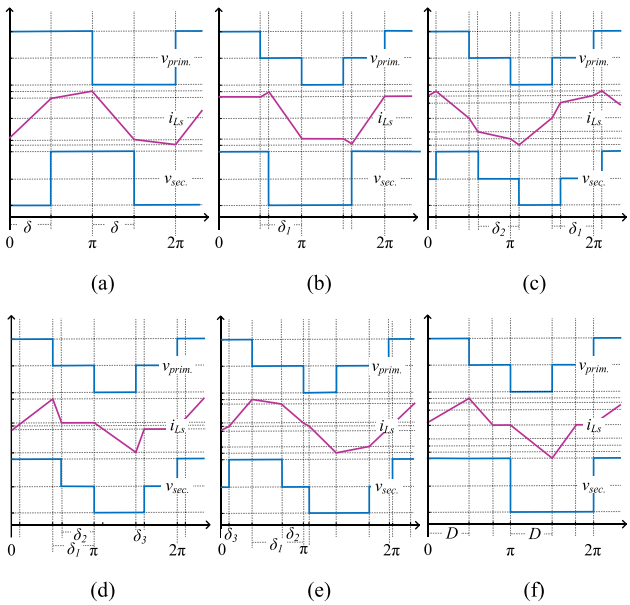

FIGURE 11. Non-resonant dual-active bridge converter modulation strategies: (a) phase-shift modulation (PSM); (b) extended phase-shift modulation (EPSM); (c) dual phase-shift (DPSM); (d) triangular triple phase-shift (TRM); (e) trapezoidal triple phase-shift (TZM); (f) pulse-width modulation (PWM). Here the current (i_{Ls}) waveforms depend on the phase angles (δ_x) and could be different according to the power processed levels.

because many single-stage and quasi-single-stage multilevel converters are based on T-type NPC. Generally, the T-type topology benefits include high efficiency and flexibility.

The power circuit of the T-type converter is presented in Fig. 9. In terms of active semiconductors, both NPC and T-type have the same number of switches and gate drives, considering that the T-type needs three fully controlled switches (Q_x). However, the T-type is more advantageous because no additional clamping diodes are required. The drawback of this topology is the need for six switches under full voltage stress, while NPC uses only switches rated for half of that stress.

Other concerns regarding the T-type converter are related to the common-mode voltage and unbalances in the dc bus voltage [90], [91], [92]. Even though references [93] and [94] have compared and demonstrated that the T-type NPC has superior efficiency, the complexity of their control and hardware results in the conventional NPCs dominating industrial applications [95].

Regarding semiconductor technology, current developments of power modules based on SiC-MOSFETs are targeted to T-type converters. This can encourage their use in new applications, including two- stage i-AFE converters, or even endorse their application in single-stage and quasi-single-stage converters [86], [87].

B. TWO-STAGE I-AFE CONVERTERS: DC-DC ISOLATED TOPOLOGIES

A dc-dc converter is required in two-stage solutions to provide galvanic isolation. The conventional isolated dc-dc converter is based on the dual-active bridge (DAB) [33], [34], [35], [36], [69]. Some industrial applications of the DAB converter include battery chargers [33], [34], [35], PSUs [69], and solid-state transformers [96].

The DAB converter is shown in Fig. 10, where two active bridges are used to provide the bidirectional power flow between different dc buses (v_1, v_2).The DAB converter can handle the bidirectional power flow, includes a low number of devices, is capable of buck-boost operation, has low sensitivity to parametric variations, and features a predictable dynamic response [97]. Also, it includes only one magnetic component – the high-frequency transformer. In some cases, an external inductor is used in series with the transformer to ensure an adequate inductance.

However, the leakage inductance (L_s) could be used as a power transfer element, and ideally, no additional magnetics are required [35].

DAB converter operation is based on modulating the voltages $v_{prim.}$ and $v_{sec.}$ in both sides of the high-frequency transformer. Various control approaches are possible, including phase-shift modulations (PSM), pulse-width (PWM), and frequency modulations (FM). According to the modulation strategies, DAB converters are divided into non-resonant (PSM, PWM) and resonant topologies (FM).

1) NON-RESONANT DUAL-ACTIVE BRIDGE CONVERTER

Non-resonant DAB converters are generally implemented based on phase-shift control, as illustrated in Fig. 11. The single phase-shift modulation (SPSM) method is presented in Fig. 11(a). PSM controls the phase angle (δ) between $v_{prim.}$ and $v_{sec.}$, considering both as square waveforms [98]. Some

advantages are obtained with PSM when both voltages are matched, ZVS-on and low circulating current at medium and high-power levels [97], [98], [99]. However, when a wide voltage gain range is needed, PSM results in a high circulating current, decreasing the converter efficiency [35], [98].

Improved modulations have been proposed to overcome these drawbacks, including the extended phase-shift (EPSM) [36], dual phase-shift (DPSM) [100], [101], and triple phase-shift modulations (TPSM) [102], [103]. The modulation strategies are based on the phase-angles between different voltages and the inner phase-shift of each active bridge: EPSM (δ_1) [see Fig. 11(b)], DPSM (δ_1, δ_2) [see Fig. 11(c)], and TPSM (δ_1, δ_2, δ_3) [see Fig. 11(d) and (e)].

TPSM is the generalized case because it controls all possible phase-angles in the DAB converter. Current research efforts in the development of TPSMs are concentrated on optimizations to properly select the correct combination of the control variables (δ_1, δ_2, δ_3) to achieve minimum conduction and/or switching losses in semiconductors. It means that no unified solution is proposed in the literature, and different objectives of optimization can be analyzed, including extension ZVS-on range, reduction of circulating and *rms* currents, improvement of the control dynamics, etc. [97]. In [97] all the aspects of DAB converter modulation and control are analyzed comprehensively.

In addition, pulse-width modulation (PWM) has been studied in recent years as an option for PSM-based DAB converters [35]. In this case, carrier-based signals are used to control the dual-active bridge. The main advantage is its simplicity because it is possible to obtain a wide ZVS-on range with only one control variable – the converter duty cycle [35]. This assumption makes the converter design less complex when compared with PSM-based DAB [106], [107]. However, PWM-based DAB suffers from asymmetrical losses and high *rms* current, which is a disadvantage in terms of the converter lifetime and efficiency [35], [107]. Reference [35], for example, uses PWM only at light loads when these strategies cannot attain their advantages. PSM strategies are still most widely used for high power levels because of the highest efficiency.

2) RESONANT DUAL-ACTIVE BRIDGE CONVERTERS

Another approach for DAB converter implementation is to include resonant cells in the topology. Typically, high-frequency resonant cells are connected with the isolation transformer to smooth their current waveform [3], [69], [108], [109], [110]. The processed energy is stored in the transformer and the resonant cell, ensuring a wide soft-switching range. Even though this is a hardware solution, in resonant DAB converters, it is possible to obtain higher efficiency because they do not have the compromise between ZVS-on and *rms* current [108], [109], [110]. This is a significant advantage when comparing resonant topologies with non-resonant converters, where the ZVS loss is a serious problem.

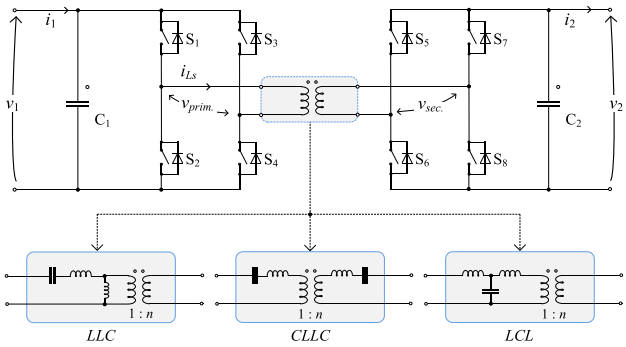

FIGURE 12. Resonant cells applied in conventional dual-active bridge converters, including the *LLC* cell, *CLLC*, and *LCL*, highlighted in the power converter circuits.

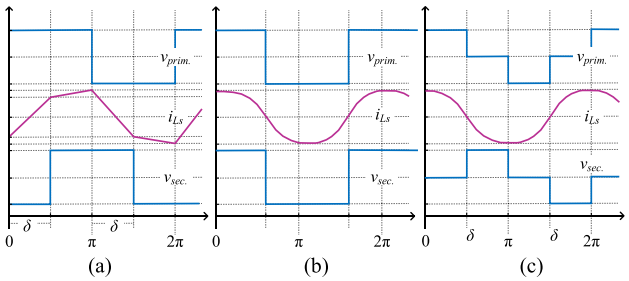

FIGURE 13. Comparison of non-resonant and resonant dual-active bridge converters: (a) non-resonant DAB converter based on phase-shift modulation; (b) resonant dual-active bridge based on two-level voltages; (c) resonant dual-active bridge based on three-level voltages.

In industrial applications, the *LLC* topology is often applied in PSUs and datacenters [69]. Fig. 12 presents the power circuit of the resonant DAB converter, highlighting the possible resonant cells, *LLC*, *CLLC,* and *LCL*, which could be advantageous to achieve application-specific requirements.

Fig. 13 compares non-resonant and resonant waveforms. For non-resonant topologies, the current waveform is typically close to square-wave, trapezoidal, or triangular [see Fig. 13]. For resonant topologies, the transformer current (i_{Ls}) is typically sinusoidal or quasi-sinusoidal [see Fig. 13]. This is another advantage of resonant converters – avoiding high *di/dt* values reduces electromagnetic interferences.

The control flexibility of resonant converters is typically limited since they are regulated by frequency variations [35], [97]. This decreases their capability to regulate the output voltage and limits the voltage conversion ratio, which is not the case for non-resonant converters (PSM and PWM-based) [35]. Additionally, the resonant frequency depends on the cell and isolation transformer parameters. Therefore, the converter efficiency is sensitive to parametric variations, which can occur due to operating temperatures and changes in component parameters during the lifetime [97].

Both resonant and non-resonant DABs are designed to operate with high frequencies, where Si and SiC semiconductors can be applied. Currently, high-power SiC devices

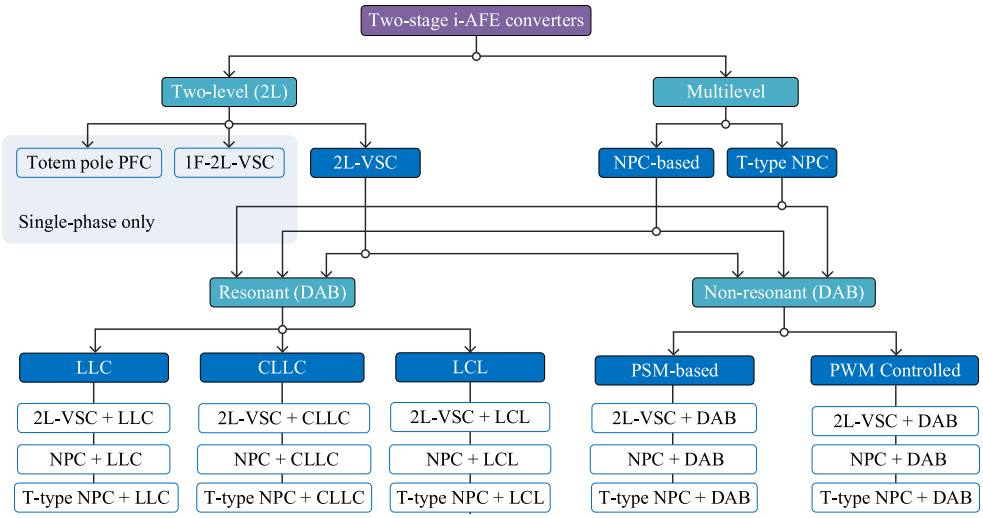

FIGURE 14. Classification of two-stage i-AFE converters according to the possible topologies for the PFC stage and isolated dc-dc.

have been used to improve the conversion efficiency. However, for low-voltage levels, GaN switches are appearing in many applications and are becoming a future trend to improve efficiency and power density [69], [70].

C. CLASSIFICATION OF TWO-STAGE I-AFE CONVERTERS

Two-stage i-AFE converters have been adopted for different applications, from low-voltage and low-power [6], [69], [70], [79], [80], [81], [82], [83], [84], [85] to high-voltage and high-power levels [86], [87], [112]. To establish a point of reference for future research, this paper proposes a classification of existing topologies. Following the general classification of i-AFE converters presented in Fig. 6, possible combinations of PFC and dc-dc stages can be divided according to the number of voltage levels at the ac side and between resonant or non-resonant topologies at the dc side. The proposed classification is presented in Fig. 14.

In industrial applications, the dual-active bridge is predominant on the dc side. That is why the i-AFE converters can also be classified according to the modulation strategy used in the isolation stage.

As mentioned, the resonant DAB topologies (*LLC*, *CLLC*, and *LCL*) are typically controlled by frequency variation. In contrast, for non-resonant topologies, the modulation strategies are divided between PSM (SPSM, DPSM, and TPSM) and PWM.

For the PFC stage, the totem-pole PFC and single-phase 2L-VSC (1F-2L-VSC) are well known and widely spread in many low-power applications. However, these topologies are limited to single-phase systems, while dc microgrids and nanogrids are commonly based on three-phase systems.

For three-phase systems, the 2L-VSC converter is currently the most used PFC topology. The advantages of using a 2L-VSC include simplicity and a low number of components. However, for high-power levels, the 3L-NPC has advantages in terms of voltage stress and power quality. For example, [112] proposes an NPC+DAB for a high-power hybrid PV system. To exemplify the two-stage solutions, Fig. 15 presents an i-AFE converter based on 2L-VSC in the PFC stage and a non-resonant dual-active bridge for high-frequency isolation. This topology is most widely used in industrial applications, including UPSs [113], [114], [115], on-board EV chargers [116], [117], and interlinking converters for dc nanogrids [118], [119], [120].

D. QUASI SINGLE-STAGE I-AFE CONVERTERS

In quasi-single-stage (q-SS) topologies, no evident intermediate dc bus is used, which means that the PFC and dc-dc stage are integrated without a decoupling capacitance. Some papers consider this as an advantage because the absence of a bulky capacitor can be used to increase the converter power density [27], [32], [37], [38], [39]. On the other hand, a minimum holdup time and voltage ripple are required in many applications. In these cases, the output capacitance would be necessary because of the absence of an intermediate dc bus that typically reduces the low-frequency harmonics from the PFC stage [121].

For two-level topologies, the leading solutions for q-SS i-AFE converters are based on bridge converters and their variations. In contrast, the multilevel topologies include the T-type NPC for the PFC stage [37], [38], [39], [121].

1) TWO-LEVEL Q-SS I-AFE CONVERTERS

The reference configuration for two-level q-SS converters is based on 2L-VSC as the PFC, and non-resonant DAB for the isolated dc-dc stage – such as the two-stage solution presented in Fig. 15 [122]. The main difference between two-stage and q-SS topologies is the absence of a decoupling dc bus. Hence, the high-frequency dynamics of the PFC and dc-dc stages are not decoupled. Therefore, the PFC and isolated stage must be grouped and analyzed for the implementation of a cooperative

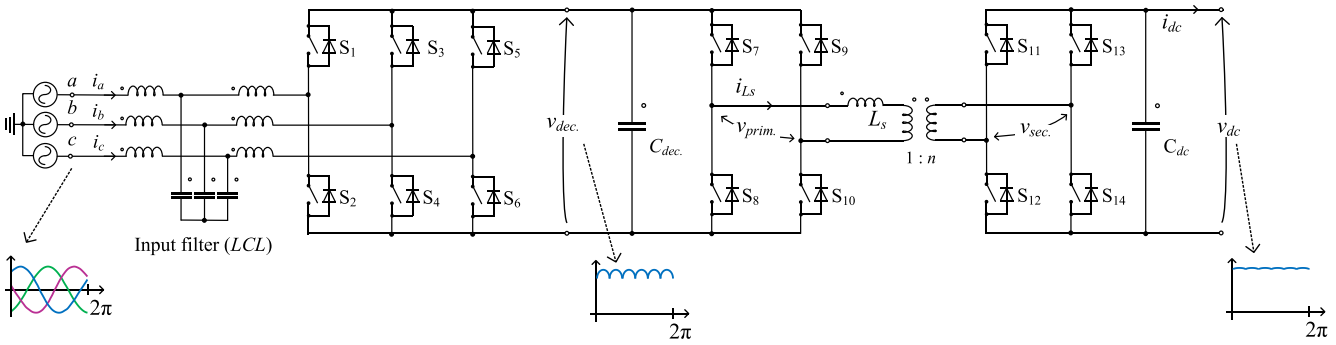

FIGURE 15. Power circuit of the two-stage i-AFE converter based on a two-level voltage source converter and non-resonant dual-active bridge (2L-VSC + DAB).

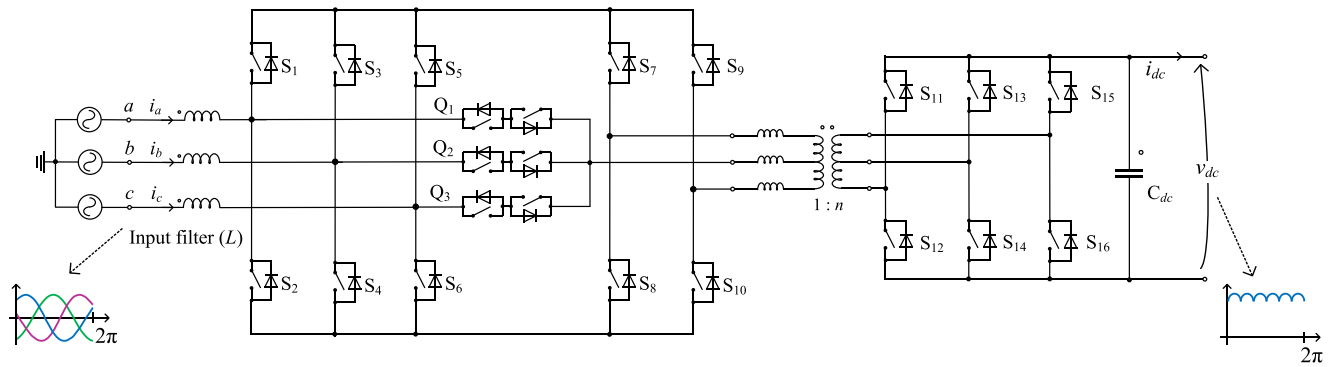

FIGURE 16. Power circuit of the quasi-single-stage i-AFE converter based on the T-type and full-bridge converter used to allow operation with a three-phase transformer.

modulation strategy [122]. As a result, the modulation is typically more complex for the q-SS. At the same time, two-stage solutions can be controlled using well-known strategies, for example, simple carrier-based modulations for the PFC stage and PSM for the DAB converter [88].

Reference [122] classifies these topologies according to the number of switch bridges used in each power processing stage. For example, a three-phase 2L-VSC includes one leg per phase, while a single-phase dual-active bridge needs four more to handle the bidirectional power flow. In total, this results in a seven-leg q-SS converter [38], [123]. In terms of practical developments, even though reference [122] proposes three-phase solutions for the ac side, the single-phase six-leg q-SS converter is the most common and well-developed solution that has experimental validation for many applications [38], [124], [125]. For i-AFE converters, the current developments are targeting mostly multilevel T-type converters.

2) T-TYPE QUASI-SINGLE-STAGE I-AFE CONVERTERS

It should be noted that there are not many types of suitable multilevel topologies for q-SS i-AFE converters. The common approach taken to implement multilevel q-SS converters is based on the T-type NPC converter connected with a central-tap transformer or two single-phase transformers [46], [48], [47], [48], [49], [50], [126], [127], [128]. For single-phase transformers, the dc-dc stage is based on a half-bridge converter. For the three-phase case, a full-bridge circuit is required, and the T-type is connected in the third winding [see Fig. 16].

Half-bridge implementation has advantages in terms of component count and simplicity because the transformer design is less complex and does not require additional controllers. With three-phase transformers, it is necessary to balance their voltages to limit the circulating current in the clamping switches (Q_1-Q_3) [48], [49], [50]. On the other hand, it should be noted that half-bridge converters are naturally limited in their power processing capability. For high-power levels, full-bridge converters are preferred [126], [127], [128]. In addition, references [129] and [130] propose the T-type+full-bridge topology to provide fault tolerance. Even though this increases the number of semiconductors in the isolation stage, it increases the power processed and allows one to arrange the high-frequency transformer in different ways. Different connections of the transformer windings can improve the converter voltage ratio, allowing their usage in various applications. For example, it is necessary to boost the input voltage [46], [47].

Fig. 17 illustrates the different transformer connections, which include [Y-Δ], [Δ-Δ], [Δ-Y], and [Y-Y]. The

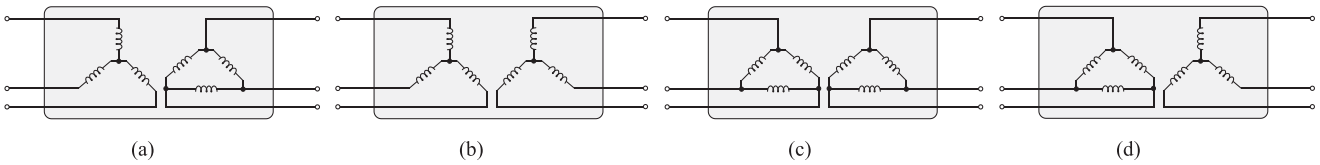

FIGURE 17. Possible connections for the high-frequency transformer in the three-phase dual-active bridge converter: (a) Y-Δ; (b) Y-Y; (c) Δ -Δ; (d) Δ-Y.

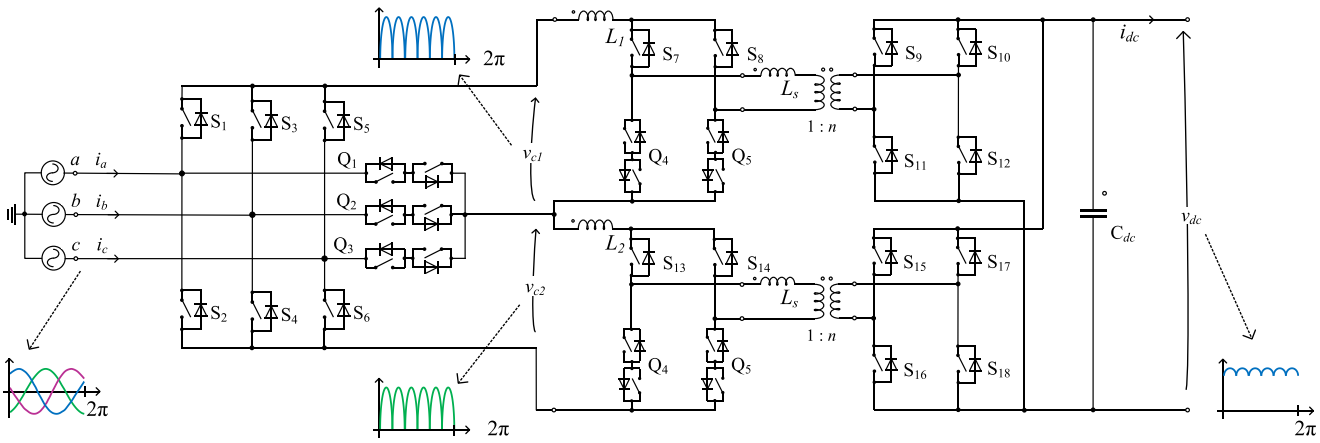

FIGURE 18. Power circuit of an unfolder quasi-single-stage i-AFE converter based on the T-type and current-fed dual-active bridge.

connection depends on the application objectives – either boost or buck the input voltage. The main advantage of three-phase transformers is that the effective frequency of the transformer voltage is higher than the switching frequency, resulting in the transformer size reduction [122].

A drawback of the multilevel q-SS is related to the direct connection between the PFC and the isolation transformer. In several applications, ac filters are formed by *L* or *LCL* filters, resulting in a current-fed solution from the input side at ac [see Fig. 16]. Due to the direct interaction between an ac filter and a high-frequency transformer, overvoltage problems are common during the turn-off of semiconductors [33]. In some cases, these overvoltages can be attenuated by the modulation strategy. Otherwise, hardware solutions, such as snubber capacitors or bidirectional active clamps, are necessary [128].

3) UNFOLDING QUASI-SINGLE STAGE I-AFE CONVERTERS

The last option to implement multilevel quasi-single-stage converters is based on unfolder-based solutions, with parallel converters on the dc side [131], [132], [133], [134], [135]. In these cases, the ac-dc stage can be implemented with NPC [136], [137] or T-type converters [135], and the neutral point is not directly connected to the transformer windings. Fig. 18 shows an example considering the T-type converter for the ac-dc stage. The resulting neutral point is connected to two series current-fed DAB converters on the dc side.

The dc-dc stage preferably should be current-fed to control the power-factor [135]. This allows the switches on the ac-dc stage to operate at low frequency, reducing switching losses [134]. The result is that each power stage can be controlled individually, significantly simplifying the modulation schemes. In addition, no low-frequency filters are needed on the ac side; thus, the number of magnetic components is reduced and the overall system efficiency is improved [133], [135].

Due to the low losses and high-efficiency, the ac-dc stage can be implemented for high power levels mainly on the ac side. For the dc side, it is possible to divide the rated power between dc-dc submodules, increasing the overall system efficiency [131], [132], [133].

One advantage of unfolding solutions is related to the dimensioning of semiconductors. Considering that the ac-dc converter operates at low frequency, it is possible to avoid high-speed switches for the ac side. For example, it is possible to use slow-speed IGBTs with low saturation voltage in the ac-dc converter, while the dc-dc could be implemented with fast SiC-MOSFETs [135]. In the T-type-based q-SSs, both stages operate at high frequency, limiting semiconductor choices due to the presence of switching losses [126], [127], [128].

An essential drawback of unfolder-based solutions is the number of active devices. As this solution employs more than one dc-dc conversion module, semiconductor count and driver circuits increase significantly. Hence, their application is limited to specific cases, e.g., on-board chargers [135] and modular EV charging stations [134].

E. CLASSIFICATION OF QUASI-SINGLE-STAGE I-AFE CONVERTERS

The number of topologies found in the existing literature for q-SS i-AFE converters is limited because many options

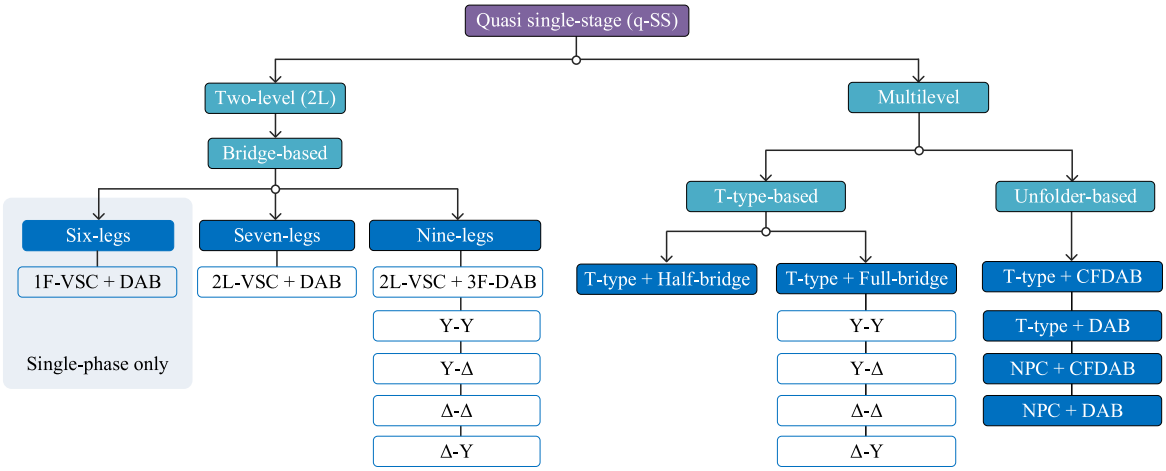

FIGURE 19. **Classification of the main topologies of quasi-single-stage i-AFE converters.**

for multilevel converters are not able to operate without an intermediate dc bus. This results in complex modulation and control schemes due to the combined PFC and dc-dc stages. Even though the unfolder solutions can reduce these issues, they are limited due to the highest number of components. This means that their application is restricted, and very specific in many cases [135].

Main approaches for two-level topologies have been developed for single-phase systems, which is a limitation to applying them as i-AFE converters. The 2L q-SS converters were also proposed; however, they have not been experimentally evaluated until this moment.

To classify the different topologies found in the literature, the ac voltage levels are used again. Additionally, the different transformer connections presented can be used to improve the voltage conversion ratio in accordance with the application needs. Fig. 19 shows the proposed classification.

F. SINGLE-STAGE I-AFE CONVERTERS

Before introducing the single-stage (SS) i-AFE converters, it is necessary to highlight the differences between the q-SS and the SS topologies. While the q-SS has well-defined PFC and dc-dc stages, the SS i-AFE converters integrate the PFC and isolation stages without clear separation. In addition, in the q-SS topologies, even without the intermediate dc bus, the input power is still processed twice [38].

Even though these SS solutions are still under development, in the last years, several topologies have been proposed, including matrix-based converters, phase-controlled, interleaved, and single-stage T-type. This subsection focuses on the analysis and characterization of these emerging solutions.

1) MATRIX-BASED DUAL-ACTIVE BRIDGE CONVERTERS

The SS i-AFE converters are mainly derived from the matrix-based DAB converter. Matrix converters or cyclo-converters were first introduced for single-stage ac-ac conversion in electric drives [88]. In the last years, this idea has been considered for isolated ac-dc conversion replacing simple semiconductors with fully controlled four-quadrant ones (Q_x) [39], [40], [41], [42], [43], [44]. To implement fully controlled switches, commonly, anti-series semiconductors are used. Fig. 20(a) shows the power circuit of the matrix-based DAB, where the first active bridge of the conventional DAB is replaced by a matrix converter with fully controlled switches (Q_1-Q_6) [37].

Regarding modulation strategies, reference [138] analyzes different switching patterns for the matrix-based DAB converter. The authors conclude that the staircase-type modulation – also called Type-A in [138] – is the optimal solution because it ensures ZVS-on for a wide operating range. In this strategy, the primary line-to-line voltage with the highest value is selected at the ac side, followed by the second largest absolute value; finally, the third step results in zero voltage. Fig. 20(b) shows the key waveforms of Type-A modulation. In addition, references [139], [140], [141], [142] propose quasi-resonant modulations, which means that matrix-based DAB converters can be divided into quasi-resonant and non-resonant topologies. An example of quasi-resonant modulation is presented in Fig. 20(c).

The difference between quasi-resonant and resonant converters is that in quasi-resonant approaches, short resonance occurs only during switching moments and not during the whole switching period [see Fig. 20(c)]. This means that quasi-resonant converters typically operate with a fixed switching frequency.

The matrix-based DAB converters are commonly supplied with a second order (*LC*) filter, resulting in a voltage-fed converter at the ac side [39], [40], [41], [42], [43], [44], [45], [46], [47], [48]. This feature is interesting when it is necessary to step down the input voltage. In addition, this avoids voltage spikes inherent in current-fed topologies. Current-fed matrix-based DAB converters with quasi-resonant modulations are described in [139] and [141]. In terms of semiconductor technology, matrix-based DAB converters are implemented with SiC-MOSFETs in several papers [39], [40], [41], [42], [43], [44], [45], [46], [47], [48], [143], and GaN power devices have been considered in recent developments [143], [144].

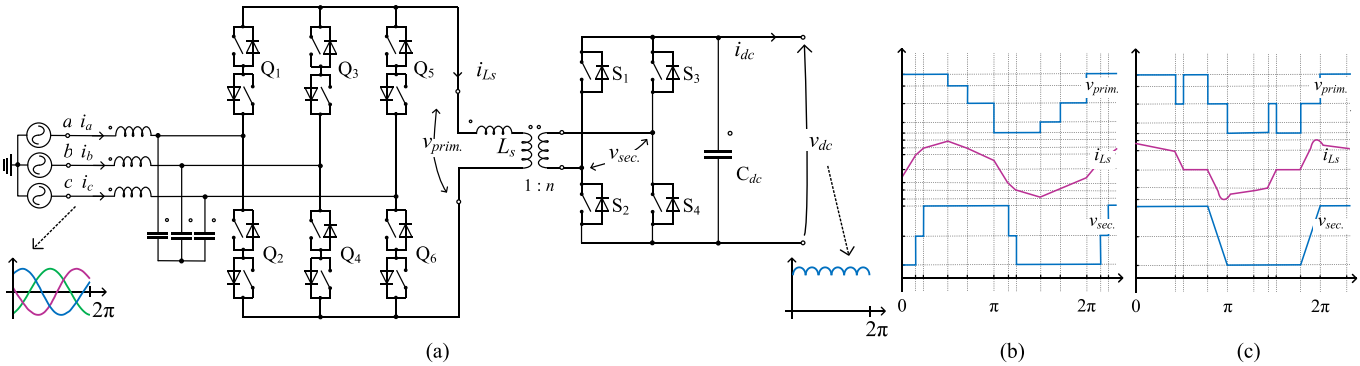

FIGURE 20. Power circuit and examples of modulation strategies of the matrix-based dual-active bridge:(a) the power circuit where the first active bridge of the conventional DAB is replaced by the matrix converter with fully controlled semiconductors (Q_x); (b) the Type-A pattern to modulate the matrix-based DAB converter; (c) a quasi-resonant modulation.

Compared with similar two-stage solutions, matrix-based DAB converters require more semiconductors, as six fully controlled switches are required. For the 2L-VSC+DAB i-AFE converter [see Fig. 15], 14 active semiconductors are necessary, while the matrix-based DAB i-AFE converter [see Fig. 20] requires 16. This issue could be mitigated when commercially available integrated bidirectional switches emerge on the market. In terms of the efficiency and power losses, both solutions are comparable because the processed *rms* current is lower in the single-stage matrix-based DAB converters. For classification purposes, matrix-based converters are commonly divided according to the number of active legs. For example, the three-phase converter exemplified in Fig. 20 is called as 3 × 2 matrix [39], [40], [41], [42], [43], [44], [45], [46], [47], [48]. Other examples are 1 × 2 and 2 × 2 matrix converters, which are the single-phase solutions [145], [146], [147], [148].

2) PHASE-CONTROLLED SINGLE-STAGE I-AFE

Another approach to implement single-stage i-AFEs is related to phase-controlled converters. These topologies are based on configurations that can operate as single-phase converters, e.g., matrix-based 1 × 2 and 2 × 2. This means that three individually controlled converters must be used in the three-phase PFC stage. Even though three-phase systems based on matrix converters were proposed in [30] and [147], this is not a common solution for i-AFE because of the high number of active components. For example, a phase-controlled i-AFE based on three 2 × 2 matrix converters results in the use of 36 active semiconductors [147], [148]. To reduce the number of components in phase-controlled solutions, SEPIC-based [149], [150], and cascaded full-bridge converters [151], [152], [153] were proposed.

The SEPIC-based i-AFE converter has advantages in terms of semiconductor count because only two switches are used per phase. The drawback of the SEPIC-based i-AFE is related to the limited power handling capability. In practical applications, the SEPIC topology increases the size of magnetic components, reducing the efficiency and power density. As a result, the SEPIC-based i-AFEs are suitable only for low-power levels, which limits their use in i-AFEs. Reference [149] presents the design and experimental evaluation of a 1.6 kW prototype. The experimental results demonstrate that the maximum efficiency occurs at medium power, being reduced considerably at the rated power.

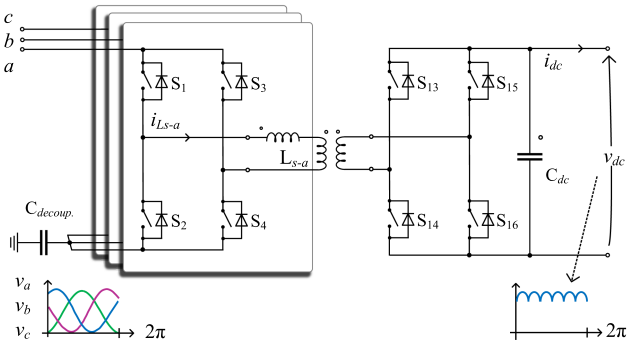

FIGURE 21. Power circuits of the three-phase single-stage cascaded full-bridge i-AFE converter.

Cascaded converters provide increased power processing capability. In this case, a decoupling capacitor is added to create an offset voltage in the neutral line [see Fig. 21]. The capacitor voltage must be controlled by the common-mode current and is required to allow direct connection between each cascaded power module. This voltage offset allows for use of generic semiconductors instead of four-quadrant switches, significantly reducing the number of semiconductor components.

3) MULTILEVEL SINGLE-STAGE TOPOLOGIES

Although the options are limited, multilevel topologies for single-stage converters have also been proposed. The main possibilities are divided between T-type NPC [46], [49] and interleaved converters, where magnetically coupled legs are used [154], [155], [156], [157], [158], [159]. Both solutions are applicable at high-power levels.

The interleaved converter presented in Fig. 22 uses coupled inductors to divide the current stress between parallel legs [154], [155], [156]. In the interleaved topology, the isolation

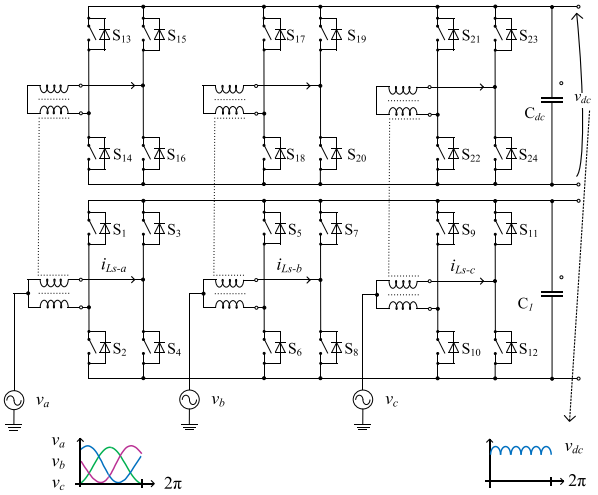

FIGURE 22. Power circuit of the three-phase single-stage cascaded full-bridge i-AFE converter.

transformer and coupled inductors could be integrated on the same magnetic core [157], [158], [159]. This means that the design of the coupled inductors could be quite complex. This complexity is also extended to the modulation and control strategies because it is necessary to avoid circulating current between parallel legs. The circulating currents result from unbalances between the processed currents of each coupled leg. Therefore, each leg must be monitored individually, which results in a high number of sensors [148].

As for the semiconductor technology, [51] and [160] propose the use of SiC-MOSFETs, which allows the high-frequency operation at above 100 kHz. In this way, the volume of magnetic components can be reduced, improving power density compromised by the use of the coupled inductors.

The second option to implement multilevel single-stage converters is based on the T-type NPC [46], [49]. This topology is derived from the q-SS version, replacing the simple semiconductors in the T-type stage with fully controlled switches [see Fig. 23]. Regarding voltage stress, both the q-SS and tSS solutions have the same requirements. However, the processed *rms* current is reduced in the SS solutions because the input power is processed only once.

Regarding the number of semiconductors, 24 single switches for the interleaved converter, and 9 fully controlled (18 discrete) plus 6 discrete switches for the T-type NPC converter are used. Even though the single-stage T-type was implemented with Si-IGBTs in [47], SiC-MOSFETs would be a better option for future developments. One advantage of both solutions is related to the fault tolerance, because the interleaved converter is controlled individually per phase, while the T-type NPC converter naturally has fault tolerance, as presented in [129] and [130].

G. CLASSIFICATION OF SINGLE-STAGE I-AFE CONVERTERS

Similar to previous subsections, the main topologies found in the literature are classified according to the voltage levels at the ac side and between resonant and quasi-resonant topologies. Fig. 24 shows the proposed classification. Compared to the two-stage and quasi-single-stage solutions, single-stage i-AFE converters are an attractive alternative, providing potential advantages such as higher power density, reduced number of power processing stages and reduced sensing requirements, because it is possible to perform the power factor control and output voltage regulation in a single stage.

The main drawback of single-stage solutions can be attributed to relative complexity, the requirement of fully controlled (four-quadrant) switches in many cases and complex modulation strategies. Most of these shortcomings can be mitigated with the development of digital signal processors, monolithic bidirectional power semiconductor devices, and design tools.

Presently, being a well-established technology, the two-stage converters have advantages because many power modules are available for these solutions. For example, integrated semiconductors could be easily found as 2L-VSC, and 3L-ANPC power modules [86], [87], [88].

H. BENCHMARK OF CURRENT SOLUTIONS AND NEW DEVELOPMENTS

The current developments of i-AFE topologies are summarized in Table 3 along with their design parameters, voltage and power rates, semiconductors technologies, and classes according to the proposed classifications. These solutions had been developed between 1 kW and 20 kW for LVDC systems, and their applications come beyond dc microgrids/nanogrids, including PSUs, data centers, EVs, and battery chargers.

Si-MOSFETs are a current technology for choice at the highest voltage levels. In addition, GaN power devices start to appear, mainly at extra-low voltage, where they can contribute to improvement of efficiency and power density. For multilevel converters, Si-IGBTs are also possible because in these topologies, semiconductors can operate with different switching losses, according to the topology and modulation strategy.

Even though ELVDC voltages are common for many dc loads, 350 V and 380 V are previewed by standards for prosumer dc buses. This is also a common parameter for other industrial applications, from where i-AFE converters can be adapted for grid integration of dc buildings. High reliability, fault tolerance, efficiency, and low time to market are a few advantages that can be obtained by choosing a proper topology. In this sense, the two-stage i-AFE converters have advantages because the technology is widespread in industrial applications.

Related to new developments, application-tailored power modules can accelerate the future adoption of quasi-single-stage and single-stage converters. Currently, these emerging topologies remain a promising research topic that lacks broader industrial awareness. Additionally, practical realization of different topologies reveals advantages and disadvantages according to the processed power levels, semiconductor technologies, and applications. Therefore, this list

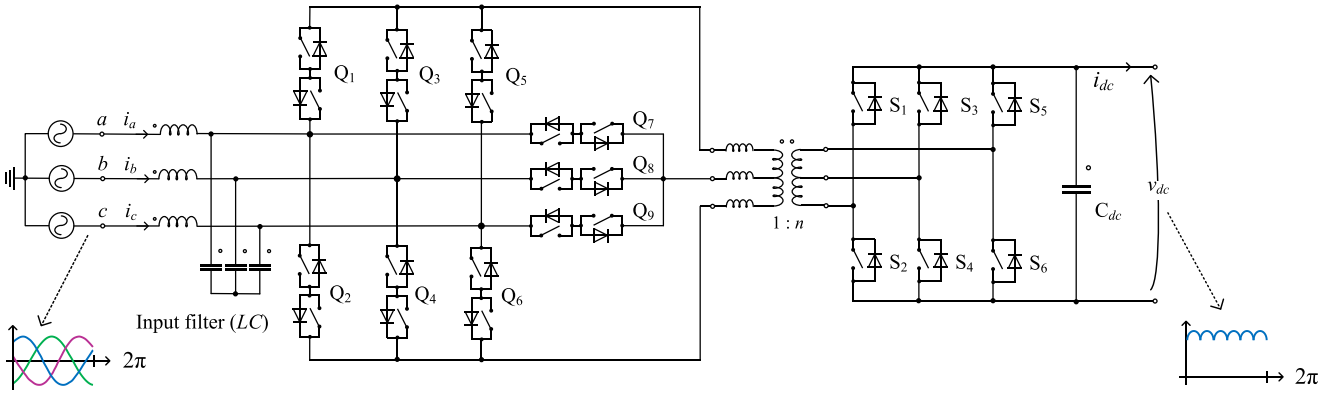

FIGURE 23. Power circuits of the three-phase single-stage T-type NPC i-AFE converter.

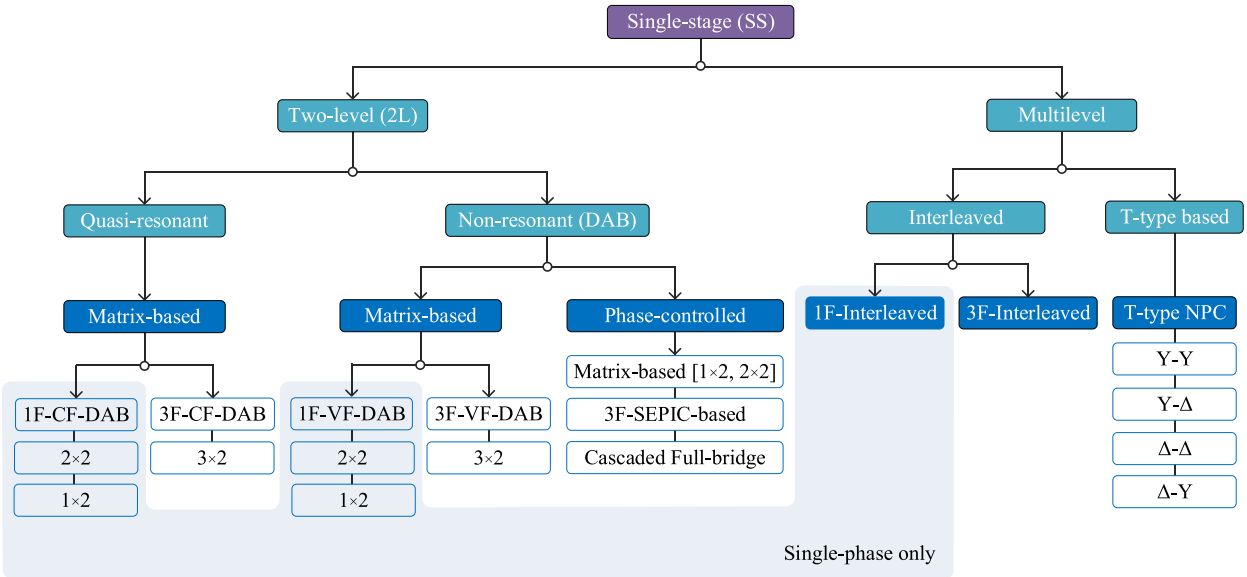

FIGURE 24. Classification of the main topologies of the single-stage i-AFE converter.

can provide values that can be an initial suggestion for practical developments.

IV. SUMMARY AND FUTURE TRENDS

Attractiveness of dc systems has motivated a series of new developments in power electronics and standardization for prosumer dc electrical installations. This is especially important for residential applications, where PV systems and energy storage can be integrated and managed closer to the end-user and more efficiently. The current standards for dc installations require an isolated interface between the ac utility grid and prosumer dc buses. This is necessary to facilitate protection and grounding schemes, increasing safety for the users.

To provide galvanic isolation, a range of topologies of i-AFE converters can be used, including two-stage, quasi-single-stage, and single-stage solutions. In this section, the main specifications of each solution will be compared.

A. IMPLEMENTATION ASPECTS OF I-AFE CONVERTERS

1) CONTROL SYSTEM

An active rectifier draws the input current in two-stage converters and regulates the intermediate dc bus voltage, requiring two control loops (PFC and VR). The dc-dc isolated stage is used to control the output voltage and the power flow between dc buses [113], [114], [115]. One alternative to simplify the control strategy is to operate the dc-dc stage in an open-loop as a dc transformer [165], controlling the output voltage through the PFC stage [69]. Fig. 25 summarizes the functionalities of each solution.

In quasi-single-stage and single-stage configurations, it is necessary to control only input current and output voltage, reducing the number of sensors and control loops. This is an advantage from the control point of view. However, the modulation strategy will be complex because both stages, PFC and isolation are integrated.

TABLE 3. Benchmark of Current Developments of Isolated Active Front-End Converters

	Classification	Configuration	REF	Technology	Freq. (f_s)	ac voltage	dc voltage	Effic. (n)	Power	Application
Two-stage	2L non-res.	Totem-pole + DAB	[70]	SiC-GaN	65 kHz	230 V*rms*	48 V*dc*	99.0 %	3 kW	PSU (data centers)
	2L non-res.	1F-2L-VSC+DAB	[6]	Si-SiC	24 kHz	127 V*rms*	380 V*dc*	95.0 %	1 kW	dc nanogrids
	2L res.	2L-VSC+LLC	[69]	SiC-GaN	250-450 kHz	230 V*rms*	48 V*dc*	99.0 %	3 kW	Data centers
	2L res.	2L-VSC+CLLC	[109]	Si-MOSFET	100 kHz	230 V*rms*	380 V*dc*	98.0 %	6 kW	dc microgrids
	2L res.	2L-VSC+CL	[144]	SiC-GaN	500 kHz	230 V*rms*	450 V*dc*	97.2 %	7 kW	EV charger
	2L non-res.	2L-VSC+DAB	[113]	Si-MOSFET	20 kHz	127 V*rms*	400 V*dc*	–	1 kW	hybrid PV systems
	2L non-res.	2L-VSC+DAB	[83]	SiC-MOSFET	100 kHz	230 V*rms*	800 V*dc*	97 %	6 kW	isolated PFC
	3L non-res.	3L-NPC+DAB	[112]	Si-IGBT	5 kHz	127 V*rms*	1200 V*dc*	–	3.4 kW	hybrid PV systems
	3L non-res.	T-type+DAB	[161]	Si-MOSFET	25 kHz	230 V*rms*	330 V*dc*	–	10 kW	EV charger
Quasi-single-stage	2L non-res.	6 bridges	[162]	Si-MOSFET	160 kHz	230 V*rms*	28 V*dc*	97.5 %	1 kW	energy storage
	2L non-res.	7 bridges	[123]	Si-MOSFET	43.2 kHz	220 V*rms*	40 V*dc*	91.0%	1 kW	energy storage
	2L non-res.	9 bridges	[122]	–	20 kHz	260 V*rms*	196 V*dc*	–	3 kW	dc microgrids
	3L non-res.	T-type+half-bridge	[46]	Si-IGBT	20 kHz	260 V*rms*	380 V*dc*	91.0 %	3 kW	dc microgrids
	3L non-res.	T-type+full-bridge	[50]	Si-IGBT	20 kHz	260 V*rms*	380 V*dc*	93.0 %	3 kW	dc microgrids
Single-stage	2L res.	1×2 matrix-based	[163]	SiC-MOSFET	50 kHz	230 V*rms*	240 V*dc*	94.5 %	1.5 kW	energy storage
	2L res.	2×2 matrix-based	[141]	SiC-MOSFET	50 kHz	230 V*rms*	48 V*dc*	95.0 %	1.2 kW	energy storage
	2L res.	3×2 matrix-based	[164]	SiC-MOSFET	100 kHz	230 V*rms*	350 V*dc*	–	5 kW	dc microgrids
	2L non-res.	1×2 matrix-based	[145]	Si-MOSFET	100 kHz	220 V*rms*	60 V*dc*	91.0 %	1 kW	dc nanogrids
	2L non-res.	2×2 matrix-based	[142]	SiC-MOSFET	50 kHz	230 V*rms*	400 V*dc*	95.0 %	3 kW	on-board EV charger
	2L non-res.	3×2 matrix-based	[39]	SiC-MOSFET	25-60 kHz	230 V*rms*	400 V*dc*	99.0 %	8 kW	isolated PFC
	2L non-res.	3×2 matrix-based	[40]	Si-IGBT	10 kHz	115 V*rms*	400 V*dc*	82.1 %	1.6 kW	EV charger (V2G)
	2L non-res.	3×2 matrix-based	[44]	SiC-MOSFET	20 kHz	230 V*rms*	400 V*dc*	–	10 kW	energy storage
	2L non-res.	3×2 matrix-based	[45]	SiC-MOSFET	20 kHz	200 V*rms*	230 V*dc*	96.5 %	1 kW	dc microgrids
	2L non-res.	Phase-controlled 1×2	[30]	SiC-MOSFET	20-100 kHz	230 V*rms*	200 V*dc*	96.0 %	2.2 kW	dc microgrids
	2L non-res.	Phase-controlled 1×2	[166]	Si-MOSFET	10 kHz	140 V*rms*	400 V*dc*	–	8 kW	SST
	2L non-res.	3F-SEPIC-based	[149]	Si-MOSFET	50 kHz	200 V*rms*	120 V*dc*	91.5 %	1.6 kW	dc microgrids
	2L non-res.	Cascaded full-bridge	[153]	SiC-MOSFET	45 kHz	230 V*rms*	375 V*dc*	–	20 kW	dc microgrids
	3L non-res.	1F-Interleaved	[160]	SiC-MOSFET	50 kHz	220 V*rms*	400 V*dc*	92.5 %	1 kW	dc microgrids
	3L non-res.	3F-Interleaved	[51]	SiC-MOSFET	50 kHz	270 V*rms*	380 V*dc*	92.5 %	5 kW	dc microgrids
	3L non-res.	T-Type NPC	[47]	Si-IGBT	20 kHz	260 V*rms*	196 V*dc*	–	2.4 kW	dc microgrids

*n: peak efficiency.

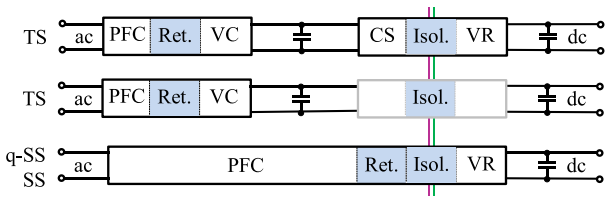

FIGURE 25. Distribution of the main tasks required to perform i-AFE conversion, including the power factor correction (PFC), intermediate dc bus voltage control (VC), and voltage regulation (VR) for the output [167].

2) NUMBER OF COMPONENTS

Commonly, single-stage converters have a disadvantage in the use of fully controlled switches, increasing the number of gate drives, isolated auxiliary power supplies, and discrete semiconductors. On the other hand, phase-controlled converters, such as the SEPIC-based one, can reduce this problem, but their applicability is limited. Each topology must be analyzed individually to evaluate these criteria. Fig. 26 compares the main topologies according to the number of switches.

3) AC FILTER

Commonly, single-stage converters are implemented with an *LC filter* to provide a voltage-fed feature for the ac side. Interestingly, this avoids overvoltage problems inherent in isolated current-fed converters [33].

For two-stage converters, it is not a problem due to the presence of the decoupling capacitance. Therefore, *LCL* filters are feasible, increasing the attenuation factor for low-order harmonics at the ac side. While the second-order *LC* filter

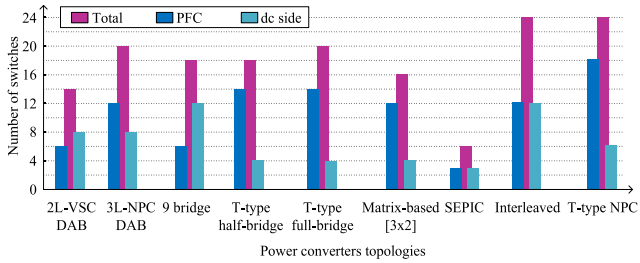

FIGURE 26. Comparison of the number of semiconductors for different i-AFE converter topologies.

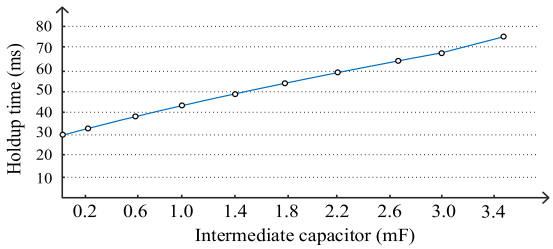

FIGURE 27. Evaluation of the holdup time considering different values for the intermediate capacitor according to the results of [121], which considers a 5 kW dc system.

results in an attenuation of –40 dB/dec, the third-order *LCL* ensures –60 dB/dec attenuation.

4) OUTPUT CAPACITANCE

Some papers advocate for single-stage solutions due to the absence of the decoupling capacitance. This can increase the converter power density in some applications [27], [32]. For dc microgrids, the total converter's capacitance is important to ensure an adequate holdup time. The minimum holdup time is defined in the IEC 61000-4-11. Reference [121] compares the holdup time for different scenarios, considering that the total capacitance can be shared between the intermediate decoupling and output capacitors.

The main results are presented in Fig. 27.According to the results of Fig. 27, the holdup time can be improved with the highest intermediate dc buses. This occurs because in two-stage solutions, the intermediate dc bus can be discharged below the voltage limits required for dc microgrids. This allows keeping the output voltage regulation during transient periods. Thus, it is possible to improve the holdup time without oversizing the total capacitance. For single-stage converters, there is no degree of freedom to increase the holdup time from the control point of view. This is potentially increasing the total capacitance, and consequently the converter becomes bulky.

B. OPPORTUNITIES FOR FURTHER RESEARCH

According to the current solutions for i-AFE converters, some opportunities for future work and research can be highlighted. This paper presents standards for dc electrical installations and electronic devices to create a background for future developments. However, to consolidate the technology, it is essential to define specific standards for i-AFE converters. This could be based on current standards from the related application fields to match the i-AFE converter design with dc microgrids and load requirements. Simultaneously, it is important to consider the i-AFE specifics to define standardization. For example, current standards do not cover the operation of AFE converters as rectifiers during UVRT and OVRT on the ac side.

For single-stage converters, the main limitation is related to the need of fully controlled switches. The development of new monolithic bidirectional power modules is necessary to overcome this problem. It can simplify the converter design and increase industrial interest in this emerging technology.

Regarding industrial developments, it is also necessary to compare the different topologies of i-AFE converters in terms of reliability. As presented in the topologies overview, there is no clear candidate for i-AFE converters. Each topology will depend strongly on the application voltage and power range. For two-stage solutions, the aspects related to reliability are quite clear because this is an industrial solution. However, quasi-single-stage and single-stage converters must be analyzed as they are primarily developed in academia and lack field data.

For the power converter topologies, new developments in the DAB converters are still emerging, including the development of multilevel and multiport converters. In the isolation stage, multilevel topologies offer advantages at high-power levels and present more degrees of freedom to improve the modulation strategy [168], [169]. Related to the multiport converters, it is necessary to note that standards like NPR9090 require galvanic isolation between prosumer (LVDC) and auxiliary dc buses at extra-low voltage levels (USB-c). Therefore, implementations of the i-AFE converters with multiport topologies can somewhat reduce the number of power processing stages [169].

C. COMPLEMENTARY LITERATURE

There are several useful references in the i-AFE field left that worth to be specifically mentioned in this paper. Therefore, they are listed below as complementary literature:

S. Rivera et al. [1]: the paper covers bipolar technologies for dc microgrids at distribution level. While this paper covers residential dc microgrids/nanogrids and their respective i-AFE converters, it can be used as a guideline for applications with higher rated power. For example, ± 350 V dc buses can be used as a bipolar system in industry-scale microgrids.

IEC Technology Report [14]: this report presents an overview of loads, technologies, and applications for dc systems and can be used as design guidelines for dc electrical installations, defining voltage and power levels, distances, requirements for cables, etc.

O. Korkh et al. [37]: the paper presents a review of isolated matrix converters for single-phase applications. For low-power levels and single-phase systems, specific topologies can be applied. In this sense, even though this review presents different applications, it can be used complementarily to the given paper.

N. Hou et al. [97] and S. Shao [98]: the papers present reviews and compare modulation and control strategies for dual-active bridge converters. Both references can be used as design guidelines for the DAB converter.

J. Yuan, et al. [84]: the paper presents a review of onboard chargers for electrical vehicles. This application also includes isolated ac-dc converters, which can be used as reference point for first developments of i-AFE converters.

V. CONCLUSION

For residential dc microgrids and nanogrids, isolated active-front end converters or i-AFE converters are the key components providing galvanic isolation and allowing for the energy exchange between prosumer electrical installations and the ac utility grid. Three classes of solutions for the implementation of i-AFE converters were identified and systematized: two-stage, quasi-single-stage, and single-stage converters.

Even though new research has been proposing single-stage solutions to improve efficiency and power density of the i-AFE converters, these advantages are not so clear when possible, requirements of standards are analyzed. At the current moment, no specific standard for i-AFE converters is available. Therefore, present paper evaluates the requirements from standards in related application areas to identify the main implementation challenges on the way to industrial adoption of i-AFEs.

Within the requirements of dc buildings and electronic devices, no clear candidates were found in the current literature to operate as i-AFE converters. Even though two-stage converters have advantages because of their wide industrial use, new developments in semiconductors and power modules potentially keep quasi-single-stage and single-stage converters promising solutions for the future. Currently, the adoption of two-stage solutions can save time to market and avoid reliability issues.

REFERENCES

[1] S. Rivera, R. Lizana F., S. Kouro, T. Dragičević, and B. Wu, "Bipolar DC power conversion: State-of-the-Art and emerging technologies," *IEEE J. Emerg. Sel. Topics Power Electron.*, vol. 9, no. 2, pp. 1192–1204, Apr. 2021, doi: 10.1109/JESTPE.2020.2980994.

[2] J. F. Martins, E. Romero-Cadaval, D. Vinnikov, and M. Malinowski, "Transactive energy: Power electronics challenges," *IEEE Power Electron. Mag.*, vol. 9, no. 1, pp. 20–32, Mar. 2022, doi: 10.1109/MPEL.2022.3140981.

[3] M. -H. Ryu, H. -S. Kim, J. -W. Baek, H. -G. Kim, and J. -H. Jung, "Effective test bed of 380-V DC distribution system using isolated power converters," *IEEE Trans. Ind. Electron.*, vol. 62, no. 7, pp. 4525–4536, Jul. 2015, doi: 10.1109/TIE.2015.2399273.

[4] D. Kumar, F. Zare, and A. Ghosh, "DC microgrid technology: System architectures, AC grid interfaces, grounding schemes, power quality, communication networks, applications, and standardizations aspects," *IEEE Access*, vol. 5, pp. 12230–12256, 2017, doi: 10.1109/ACCESS.2017.2705914.

[5] D. Boroyevich, I. Cvetkovic, R. Burgos, and D. Dong, "Intergrid: A future electronic energy network?," *IEEE J. Emerg. Sel. Topics Power Electron.*, vol. 1, no. 3, pp. 127–138, Sep. 2013, doi: 10.1109/JESTPE.2013.2276937.

[6] E. L. Carvalho, L. V. Bellinaso, R. Cardoso, and L. Michels, "Distributed price-based power management for Multi-buses DC nanogrids EEMS," *IEEE J. Emerg. Sel. Topics Power Electron.*, vol. 10, no. 5, pp. 5509–5521, Oct. 2022, doi: 10.1109/JESTPE.2022.3152101.

[7] *IEC Low-voltage electrical installations – Part 8-2: Prosumer's low-voltage electrical installations*, IEC Standard 60364-8-2, 2018.

[8] T. Dragičević, X. Lu, J. C. Vasquez, and J. M. Guerrero, "DC microgrids—Part I: A review of control strategies and stabilization techniques," *IEEE Trans. Power Electron.*, vol. 31, no. 7, pp. 4876–4891, Jul. 2016, doi: 10.1109/TPEL.2015.2478859.

[9] T. Dragičević, X. Lu, J. C. Vasquez, and J. M. Guerrero, "DC microgrids—Part II: A review of power architectures, applications, and standardization issues," *IEEE Trans. Power Electron.*, vol. 31, no. 5, pp. 3528–3549, May 2016, doi: 10.1109/TPEL.2015.2464277.

[10] M. Alshareef, Z. Lin, F. Li, and F. Wang, "A grid interface current control strategy for DC microgrids," *CES Trans. Elect. Mach. Syst.*, vol. 5, no. 3, pp. 249–256, Sep. 2021, doi: 10.30941/CESTEMS.2021.00028.

[11] H. Tian and Y. Li, "Virtual resistor based second-order ripple sharing control for distributed bidirectional DC–DC converters in hybrid AC–DC microgrid," *IEEE Trans. Power Electron.*, vol. 36, no. 2, pp. 2258–2269, Feb. 2021, doi: 10.1109/TPEL.2020.3006072.

[12] U. Vuyyuru, S. Maiti, C. Chakraborty, and E. I. Batzelis, "Universal active power control converter for DC-Microgrids with common energy storage," *IEEE Open J. Ind. Appl.*, vol. 2, pp. 21–35, 2021, doi: 10.1109/OJIA.2021.3063625.

[13] Q. Xu, N. Vafamand, L. Chen, T. Dragičević, L. Xie, and F. Blaabjerg, "Review on advanced control technologies for bidirectional DC/DC converters in DC microgrids," *IEEE J. Emerg. Sel. Topics Power Electron.*, vol. 9, no. 2, pp. 1205–1221, Apr. 2021, doi: 10.1109/JESTPE.2020.2978064.

[14] LVDC: Electricity for the 21st Century. IEC Technology Report, International Electrotechnical Commission, Geneva, Switzerland, 2017. [Online]. Available: https://www.iec.ch/basecamp/lvdc-electricity-21st-century

[15] Y. Dafalla, B. Liu, D. A. Hahn, H. Wu, R. Ahmadi, and A. G. Bardas, "Prosumer nanogrids: A cybersecurity assessment," *IEEE Access*, vol. 8, pp. 131150–131164, 2020, doi: 10.1109/ACCESS.2020.3009611.

[16] L. R. Jie and R. T. Naayagi, "Nanogrid for energy aware buildings," in *Proc. IEEE PES GTD Grand Int. Conf. Expo. Asia*, 2019, pp. 92–96, doi: 10.1109/GTDAsia.2019.8715905.

[17] J. Hu, J. Wu, X. Ai, and N. Liu, "Coordinated energy management of prosumers in a distribution system considering network congestion," *IEEE Trans. Smart Grid*, vol. 12, no. 1, pp. 468–478, Jan. 2021, doi: 10.1109/TSG.2020.3010260.

[18] E. P. Recast, "Directive 2014/35/eu of the European parliament and of the council of 26 February 2014 on the harmonisation of the laws of the member states relating to the making available on the market of electrical equipment designed for use within certain voltage limits (recast) (Text with EEA relevance)," *Official J. Eur. Union*, vol. L, no. 96, pp. 357–374, Mar. 2014.

[19] International Electrotechnical Commission, *Low-Voltage Electrical Installations – Part 1: Fundamental Principles, Assessment of General Characteristics, Definitions*, Standard IEC 60364-1:2005, International Electrotechnical Commission, 2005. [Online]. Available: https://webstore.iec.ch/publication/1865

[20] International Electrotechnical Commission, *Low-Voltage Electrical Installations – Part 4: Protection for Safety – Protection Against Electrical Shock*, Standard IEC 60364-4-41, International Electrotechnical Commission, 2017. [Online]. Available: https://webstore.iec.ch/publication/60169

[21] International Electrotechnical Commission, *Low-Voltage Electrical Installations – Part 5: Selection and Erection of Electrical Equipment – Devices for Protection for Safety, Isolation, Switching, Control and Monitoring*, Standard IEC 60364-5-53:2019, International Electrotechnical Commission 2019. [Online]. Available: https://webstore.iec.ch/publication/68215

[22] International Electrotechnical Commission, *Low-Voltage Electrical Installations – Part 7: Requirements for Special Installations of Locations – Medical Locations*, Standard IEC 60364-7-710:2021, International Electrotechnical Commission, 2021. [Online]. Available: https://webstore.iec.ch/publication/29393

[23] International Electrotechnical Commission, *Low-Voltage Electrical Installations – Part 8-1: Functional Aspects – Energy Efficiency*, Standard IEC 60364-8-1:2019, International Electrotechnical Commission, 2019. [Online]. Available: https://webstore.iec.ch/publication/33598

[24] International Electrotechnical Commission, *Low-Voltage Electrical Installations – Part 8-2: Prosumer's low-Voltage Electrical Installations*, Standard IEC 60364-8-2:2018, International Electrotechnical Commission, 2018. [Online]. Available: https://webstore.iec.ch/publication/29098

[25] International Electrotechnical Commission, *Low-Voltage Electrical Installations – Part 8-3: Functional Aspects – Operation of Prosumer's Electrical Installations*, Standard IEC 60364-8-3:2020, International Electrotechnical Commission, 2020. [Online]. Available: https://webstore.iec.ch/publication/30963

[26] *NL: DC Installations for low Voltage*, Standard NPR 9090:2018, Royal Dutch Standardization Institute (NEN), The Netherlands, Sep. 2018.

[27] D. Rothmund, T. Guillod, D. Bortis, and J. W. Kolar, "99.1% Efficient 10 kV SiC-based medium-voltage ZVS bidirectional single-phase PFC AC/DC stage," *IEEE J. Emerg. Sel. Topics Power Electron.*, vol. 7, no. 2, pp. 779–797, Jun. 2019, doi: 10.1109/JESTPE.2018.2886140.

[28] Y. Qiu, Q. Zhong, Y. Zhao, G. Wang, and L. Wang, "A method for analyzing the voltage deviation isolation performance with an application in two-stage high-frequency isolated AC-DC converters in LVDC systems," *CPSS Trans. Power Electron. Appl.*, vol. 6, no. 3, pp. 218–226, Sep. 2021, doi: 10.24295/CPSSTPEA.2021.00020.

[29] Z. Zhang, A. Mallik, and A. Khaligh, "A high step-down isolated three-phase AC-DC converter," *IEEE J. Emerg. Sel. Topics Power Electron.*, vol. 6, no. 1, pp. 129–139, Mar. 2018, doi: 10.1109/JESTPE.2017.2725821.

[30] J. Saha, N. B. Y. Gorla, A. Subramaniam, and S. K. Panda, "Analysis of modulation and optimal design methodology for half-bridge matrix-based dual-active-bridge (MB-DAB) AC–DC converter," *IEEE J. Emerg. Sel. Topics Power Electron.*, vol. 10, no. 1, pp. 881–894, Feb. 2022, doi: 10.1109/JESTPE.2021.3107500.

[31] J. Everts, "Closed-Form solution for efficient ZVS modulation of DAB converters," *IEEE Trans. Power Electron.*, vol. 32, no. 10, pp. 7561–7576, Oct. 2017, doi: 10.1109/TPEL.2016.2633507.

[32] D. Rothmund, T. Guillod, D. Bortis, and J. W. Kolar, "99% Efficient 10 kV SiC-based 7 kV/400 V DC transformer for future data centers," *IEEE J. Emerg. Sel. Topics Power Electron.*, vol. 7, no. 2, pp. 753–767, Jun. 2019, doi: 10.1109/JESTPE.2018.2886139.

[33] E. L. Carvalho, L. H. Meneghetti, E. G. Carati, J. P. da Costa, C. M. O. Stein, and R. Cardoso, "Asymmetrical pulse-width modulation strategy for current-fed dual active bridge bidirectional isolated converter applied to energy storage systems," *Energies*, vol. 13, no. 3475, pp. 1–22, Jul. 2020, doi: 10.3390/en13133475.

[34] A. Blinov, R. Kosenko, D. Vinnikov, and L. Parsa, "Bidirectional isolated current-source DAB converter with extended ZVS/ZCS range and reduced energy circulation for storage applications," *IEEE Trans. Ind. Electron.*, vol. 67, no. 12, pp. 10552–10563, Dec. 2020, doi: 10.1109/TIE.2019.2958291.

[35] E. L. Carvalho, C. A. Felipe, L. V. Bellinaso, C. M. d. O. Stein, and R. Cardoso, and L. Michels, "Asymmetrical-PWM DAB converter with extended ZVS/ZCS range and reduced circulating current for ESS applications," *IEEE Trans. Power Electron.*, vol. 36, no. 11, pp. 12990–13001, Nov. 2021, doi: 10.1109/TPEL.2021.3078734.

[36] S. Bal, D. B. Yelaverthi, A. K. Rathore, and D. Srinivasan, "Improved modulation strategy using dual phase shift modulation for active commutated current-fed dual active bridge," *IEEE Trans. Power Electron.*, vol. 33, no. 9, pp. 7359–7375, Sep. 2018, doi: 10.1109/TPEL.2017.2764917.

[37] O. Korkh, A. Blinov, D. Vinnikov, and A. Chub, "Review of isolated matrix inverters: Topologies, modulation methods and applications," *Enegies*, vol. 13, no. 2394, pp. 1–30, May 2020, doi: 10.3390/en13092394.

[38] E. L. Carvalho, A. Blinov, A. Chub, and D. Vinnikov, "Overview of single-stage isolated AC-DC topologies for interfacing DC and AC grids," in *Proc. IEEE 13th Int. Symp. Power Electron. Distrib. Gener. Syst.*, 2022, pp. 1–6, doi: 10.1109/PEDG54999.2022.9923249.

[39] L. Schrittwieser, M. Leibl, and J. W. Kolar, "99% Efficient isolated three-phase matrix-type DAB buck–boost PFC rectifier," *IEEE Trans. Power Electron.*, vol. 35, no. 1, pp. 138–157, Jan. 2020, doi: 10.1109/TPEL.2019.2914488.

[40] D. Das, N. Weise, K. Basu, R. Baranwal, and N. Mohan, "A bidirectional soft-switched DAB-Based single-stage three-phase AC–DC converter for V2G application," *IEEE Trans. Transp. Electrific.*, vol. 5, no. 1, pp. 186–199, Mar. 2019, doi: 10.1109/TTE.2018.2886455.

[41] X. Li, F. Wu, G. Yang, H. Liu, and T. Meng, "Dual-Period-Decoupled space vector phase-shifted modulation for DAB-Based three-phase single-stage AC–DC converter," *IEEE Trans. Power Electron.*, vol. 35, no. 6, pp. 6447–6457, Jun. 2020, doi: 10.1109/TPEL.2019.2950059.

[42] F. Wu, X. Li, G. Yang, H. Liu, and T. Meng, "Variable switching periods based space vector phase-shifted modulation for DAB based three-phase single-stage isolated AC–DC converter," *IEEE Trans. Power Electron.*, vol. 35, no. 12, pp. 13725–13734, Dec. 2020, doi: 10.1109/TPEL.2020.2995712.

[43] F. Wu, X. Li, G. Wang, H. Liu, and Y. Dai, "Analysis of effect of grid harmonics and unbalance on DAB-Based three-phase single-stage AC–DC converter and solutions," *IEEE J. Emerg. Sel. Topics Power Electron.*, vol. 10, no. 1, pp. 1192–1202, Feb. 2022, doi: 10.1109/JESTPE.2021.3105674.

[44] D. Varajão, R. E. Araújo, L. M. Miranda, and J. A. P. Lopes, "Modulation strategy for a single-stage bidirectional and isolated AC–DC matrix converter for energy storage systems," *IEEE Trans. Ind. Electron.*, vol. 65, no. 4, pp. 3458–3468, Apr. 2018, doi: 10.1109/TIE.2017.2752123.

[45] M. A. Sayed, K. Suzuki, T. Takeshita, and W. Kitagawa, "Soft-Switching PWM technique for grid-tie isolated bidirectional DC–AC converter with SiC device," *IEEE Trans. Ind. Appl.*, vol. 53, no. 6, pp. 5602–5614, Nov./Dec. 2017, doi: 10.1109/TIA.2017.2731738.

[46] L. Gu and K. Jin, "A three-phase isolated bidirectional AC/DC converter and its modified SVPWM algorithm," *IEEE Trans. Power Electron.*, vol. 30, no. 10, pp. 5458–5468, Oct. 2015, doi: 10.1109/TPEL.2014.2378274.

[47] L. Gu and K. Peng, "A single-stage fault-tolerant three-phase bidirectional AC/DC converter with symmetric high-frequency y-δ connected transformers," *IEEE Trans. Power Electron.*, vol. 35, no. 9, pp. 9226–9237, Sep. 2020, doi: 10.1109/TPEL.2020.2974992.

[48] L. Gu, K. Jin, H. Zhu, and C. Wang, "A single-stage isolated three-phase bidirectional AC/DC converter," in *Proc. IEEE 5th Int. Symp. Power Electron. Distrib. Gener. Syst.*, 2014, pp. 1–5, doi: 10.1109/PEDG.2014.6878658.

[49] L. Gu and K. Peng, "A single-stage isolated three-phase bidirectional AC/DC converter for high power applications," in *Proc. IEEE Energy Convers. Congr. Expo.*, 2019, pp. 2850–2854, doi: 10.1109/ECCE.2019.8913131.

[50] L. Gu and K. Jin, "A three-phase bidirectional AC/DC converter with y–δ connected transformers," *IEEE Trans. Power Electron.*, vol. 31, no. 12, pp. 8115–8125, Dec. 2016, doi: 10.1109/TPEL.2016.2517647.

[51] B. R. de Almeida, J. W. M. de Araújo, P. P. Praça, and D. de S. Oliveira, "A single-stage three-phase bidirectional AC/DC converter with high-frequency isolation and PFC," *IEEE Trans. Power Electron.*, vol. 33, no. 10, pp. 8298–8307, Oct. 2018, doi: 10.1109/TPEL.2017.2775522.

[52] International Electrotechnical Commission, *Safety of Power Converters for use in Photovoltaic Power Systems-Part 1: General Requirements*, Standard IEC 62109-1:2010, International Electrotechnical Commission, 2010. [Online]. Available: https://webstore.iec.ch/publication/6470

[53] International Electrotechnical Commission, *Safety of Power Converters for use in Photovoltaic Power Systems-Part 2: Particular Requirements for Inverters*, Standard IEC 62109-2:2011, International Electrotechnical Commission, 2011. [Online]. Available: https://webstore.iec.ch/publication/6471

[54] International Electrotechnical Commission, *Uninterruptible Power Systems (UPS) - Part 1: Safety Requirements*, Standard IEC 62040-1:2017, International Electrotechnical Commission, 2017. [Online]. Available: https://webstore.iec.ch/publication/69012

[55] International Electrotechnical Commission, *Effects of Current on Human Beings and Livestock–Serie*, Standard IEC 60479 series, International Electrotechnical Commission, 2020. [Online]. Available: https://webstore.iec.ch/publication/62980

[56] International Electrotechnical Commission, "Uninterruptible power systems (UPS)–Part 2: Electromagnetic compatibility (EMC) requirements," Standard IEC 62040-2:2016, International Electrotechnical Commission, 2016. [Online]. Available: https://webstore.iec.ch/publication/59482

[57] International Electrotechnical Commission, *Electromagnetic Compatibility (EMC) - Part 4-11: Testing and Measurement Techniques - Voltage Dips, Short Interruptions, and Voltage Variations Immunity*

Tests for Equipment with Input Current up to 16 A per Phase, Standard IEC 61000-4-11:2020, International Electrotechnical Commission, 2020. CoolSiC™ 1200 V SiC MOSFET Application. [Online]. Available: Notehttps://webstore.iec.ch/publication/66487

[58] International Electrotechnical Commission, *Electromagnetic Compatibility (EMC)–Part 6-3: Generic Standards–Emission Standard for Equipment in Residential Environments*, Standard IEC 61000-6-3:2020, International Electrotechnical Commission, 2020. [Online]. Available: https://webstore.iec.ch/publication/27413

[59] International Electrotechnical Commission, *Electromagnetic Compatibility (EMC)–Part 6-4: Generic Standards–Emission Standard for Industrial Environments*, Standard IEC 61000-6-4:2018, International Electrotechnical Commission, 2018. [Online]. Available: https://webstore.iec.ch/publication/62637

[60] International Electrotechnical Commission, *Uninterruptible Power Systems (UPS) - Part 5-3: DC Output UPS - Performance and Test Requirements*, Standard IEC 62040-5-3:2016, International Electrotechnical Commission, 2016. [Online]. Available: https://webstore.iec.ch/publication/26118

[61] International Electrotechnical Commission, *Electromagnetic Compatibility (EMC) - Part 3-15: Limits - Assessment of low Frequency Electromagnetic Immunity and Emission Requirements for Dispersed Generation Systems in LV network*, Standard IEC 61000-3-15:2011, International Electrotechnical Commission, 2011. [Online]. Available: https://webstore.iec.ch/publication/4148

[62] International Electrotechnical Commission, *Utility-Interconnected Photovoltaic Inverters - Test Procedure of Islanding Prevention Measures*, Standard IEC 62116:2014, International Electrotechnical Commission, 2014. [Online]. Available: https://webstore.iec.ch/publication/6479

[63] International Electrotechnical Commission, *Communication Networks and Systems for Power Utility Automation - Part 90-7: Object Models for Power Converters in Distributed Energy Resources (DER) Systems*, Standard IEC TR 61850-90-7:2013, International Electrotechnical Commission, 2013. [Online]. Available: https://webstore.iec.ch/publication/6027

[64] International Electrotechnical Commission, *Distributed Energy Resources Connection With the Grid*, Standard IEC TS 62786:2017, International Electrotechnical Commission, 2017. [Online]. Available: https://webstore.iec.ch/publication/30385

[65] Y. Neyret, "DC microgrids: Principles and benefits," dc systems white paper, 2021 [Online]. Available: www.dc.systems/assets/public/DC-Systems-White-Paper.pdf

[66] R. K. Varma, "Smart inverter functions," in *Smart Solar PV Inverters With Advanced Grid Support Functionalities*. Piscataway, NJ, USA: IEEE, 2022, pp. 35–71, doi: 10.1002/9781119214236.ch2.

[67] O. Koduri, S. D. K. Varma, and S. S. Duvvuri, "Islanding detection of utility-grid interfaced PV inverter with OVP/UVP and OFP/UFP protection relays," in *Proc. Asian Conf. Innov. Technol.*, 2021, pp. 1–5, doi: 10.1109/ASIANCON51346.2021.9544744.

[68] J. Johnson, B. Fox, K. Kaur, and J. Anandan, "Evaluation of interoperable distributed energy resources to IEEE 1547.1 using sunspec modbus, IEEE 1815, and IEEE 2030.5," *IEEE Access*, vol. 9, pp. 142129–142146, 2021, doi: 10.1109/ACCESS.2021.3120304.

[69] GaN-Based 3KW Full Bridge LLC Resonant Converter Reference Design, GaN System Inc. design reference. 2021. [Online]. Available: gansystems.com/evaluation-boards/gs-evb-llc-3kw-gs

[70] 3kW High-Efficiency CCM Bridgeless Totem Pole PFC Reference Design using GaN E-HEMTs, GaN System Inc. design reference. 2021. [Online]. Available: gansystems.com/evaluation-boards/gs-evb-btp-3kw-gs

[71] S. Lee and H. Do, "A single-switch AC–DC LED driver based on a boost-flyback PFC converter with lossless snubber," *IEEE Trans. Power Electron.*, vol. 32, no. 2, pp. 1375–1384, Feb. 2017, doi: 10.1109/TPEL.2016.2549029.

[72] A. Leon-Masich, H. Valderrama-Blavi, J. M. Bosque-Moncusí, and L. Martínez-Salamero, "A high-voltage sic-Based boost PFC for LED applications," *IEEE Trans. Power Electron.*, vol. 31, no. 2, pp. 1633–1642, Feb. 2016, doi: 10.1109/TPEL.2015.2418212.

[73] M. Pérez-Tarragona, H. Sarnago, Ó. Lucía, and J. M. Burdío, "Design and experimental analysis of PFC rectifiers for domestic induction heating applications," *IEEE Trans. Power Electron.*, vol. 33, no. 8, pp. 6582–6594, Aug. 2018, doi: 10.1109/TPEL.2017.2755367.

[74] M. Pérez-Tarragona, H. Sarnago, Ó. Lucía, and J. M. Burdío, "Multiphase PFC rectifier and modulation strategies for domestic induction heating applications," *IEEE Trans. Ind. Electron.*, vol. 68, no. 8, pp. 6424–6433, Aug. 2021, doi: 10.1109/TIE.2020.3005096.

[75] K. Yao, J. Li, F. Shao, and B. Zhang, "Parallel fixed switching frequency CRM and DCM boost PFC converter with high power factor," *IEEE Trans. Power Electron.*, vol. 37, no. 3, pp. 3247–3258, Mar. 2022, doi: 10.1109/TPEL.2021.3118110.

[76] S. F. Lim and A. M. Khambadkone, "A simple digital DCM control scheme for boost PFC operating in both CCM and DCM," *IEEE Trans. Ind. Appl.*, vol. 47, no. 4, pp. 1802–1812, Jul./Aug. 2011, doi: 10.1109/TIA.2011.2153815.

[77] *UL Standard for Safety Inverters, Converters, Controllers and Interconnection System Equipment for Use with Distributed Energy Resources*, UL Std. 1741, 2018.

[78] *IEEE Standard for Interconnection and Interoperability of Distributed Energy Resources with Associated Electric Power Systems Interfaces*, IEEE Std. 1547-2018, 2018, doi: 10.1109/IEEESTD.2018.8332112.

[79] Q. Huang, Q. Ma, P. Liu, A. Q. Huang, and M. A. de Rooij, "99% Efficient 2.5-kW four-level flying capacitor multilevel GaN totem-pole PFC," *IEEE J. Emerg. Sel. Topics Power Electron.*, vol. 9, no. 5, pp. 5795–5806, Oct. 2021, doi: 10.1109/JESTPE.2021.3051207.

[80] M. -H. Park, J. Baek, Y. Jeong, and G. -W. Moon, "An interleaved totem-pole bridgeless boost PFC converter with soft-switching capability adopting phase-shifting control," *IEEE Trans. Power Electron.*, vol. 34, no. 11, pp. 10610–10618, Nov. 2019, doi: 10.1109/TPEL.2019.2900342.

[81] H. Belkamel, H. Kim, and S. Choi, "Interleaved totem-pole ZVS converter operating in CCM for single-stage bidirectional AC–DC conversion with high-frequency isolation," *IEEE Trans. Power Electron.*, vol. 36, no. 3, pp. 3486–3495, Mar. 2021, doi: 10.1109/TPEL.2020.3016684.

[82] E. Kim, F. Mwasilu, H. H. Choi, and J. Jung, "An observer-based optimal voltage control scheme for three-phase UPS systems," *IEEE Trans. Ind. Electron.*, vol. 62, no. 4, pp. 2073–2081, Apr. 2015, doi: 10.1109/TIE.2014.2351777.

[83] A. Mallik and A. Khaligh, "Maximum efficiency tracking of an integrated two-staged AC–DC converter using variable DC-Link voltage," *IEEE Trans. Ind. Electron.*, vol. 65, no. 11, pp. 8408–8421, Nov. 2018, doi: 10.1109/TIE.2018.2807364.

[84] J. Yuan, L. Dorn-Gomba, A. D. Callegaro, J. Reimers, and A. Emadi, "A review of bidirectional on-board chargers for electric vehicles," *IEEE Access*, vol. 9, pp. 51501–51518, 2021, doi: 10.1109/ACCESS.2021.3069448.

[85] R. Z. Scapini, L. V. Bellinaso, and L. Michels, "Stability analysis of AC–DC full-bridge converters with reduced DC-Link capacitance," *IEEE Trans. Power Electron.*, vol. 33, no. 1, pp. 899–908, Jan. 2018, doi: 10.1109/TPEL.2017.2672982.

[86] Infineon Technologies, "CoolSiC™ 1200 V SiC MOSFET application note," Manufacturing application note, 2018. [Online]. Available: www.infineon.com/dgdl/Infineon-CoolSiC_MOSFET_1200V-SiC_trench_power_device-ApplicationNotes-v01_01-EN

[87] A. C. Schittler and C. Mueller, "Loss-optimized active neutral-point clamped inverter in a lowinductive power-module design," in *Proc. PCIM Europe Digit. Days 2020; Int. Exhib. Conf. Power Electron., Intell. Motion, Renewable Energy Energy Manage.*, 2020, pp. 1–7.

[88] D. G. Holmes and T. A. Lipo, *Pulse Width Modulation For Power Converters: Principles and Practice*. Piscataway, NJ, USA/New York, NY, USA: IEEE Press/Wiley, 2003, pp. 215–258.

[89] X. Zhang, G. Tan, T. Xia, Q. Wang, and X. Wu, "Optimized switching finite control set model predictive control of NPC single-phase three-level rectifiers," *IEEE Trans. Power Electron.*, vol. 35, no. 10, pp. 10097–10108, Oct. 2020, doi: 10.1109/TPEL.2020.2978185.

[90] W. Jiang, H. Jiang, S. Liu, S. Ji, and J. Wang, "A carrier-based discontinuous PWM strategy for T-Type three-level converter with reduced common mode voltage, switching loss, and neutral point voltage control," *IEEE Trans. Power Electron.*, vol. 37, no. 2, pp. 1761–1771, Feb. 2022, doi: 10.1109/TPEL.2021.3106767.

[91] H. Peng et al., "Improved space vector modulation for neutral-point balancing control in hybrid-switch-based T-type neutral-point-clamped inverters with loss and common-mode voltage reduction," *CPSS Trans. Power Electron. Appl.*, vol. 4, no. 4, pp. 328–338, Dec. 2019, doi: 10.24295/CPSSTPEA.2019.00031.

[92] X. Xu, Z. Zheng, K. Wang, B. Yang, and Y. Li, "A carrier-based common-mode voltage elimination method for back-to-back three-level NPC converters," *IEEE Trans. Power Electron.*, vol. 37, no. 3, pp. 3040–3052, Mar. 2022, doi: 10.1109/TPEL.2021.3112697.

[93] M. Schweizer and J. W. Kolar, "Design and implementation of a highly efficient three-level T-Type converter for low-voltage applications," *IEEE Trans. Power Electron.*, vol. 28, no. 2, pp. 899–907, Feb. 2013, doi: 10.1109/TPEL.2012.2203151.

[94] H. Shin, K. Lee, J. Choi, S. Seo, and J. Lee, "Power loss comparison with different PWM methods for 3L-NPC inverter and 3L-T type inverter," in *Proc. Int. Power Electron. Appl. Conf. Expo.*, 2014, pp. 1322–1327, doi: 10.1109/PEAC.2014.7038054.

[95] S. Cailhol, P. -E. Vidal, and F. Rotella, "A generic method of pulsewidth modulation applied to three-phase three-level T-Type NPC inverter," *IEEE Trans. Ind. Appl.*, vol. 54, no. 5, pp. 4515–4522, Sep./Oct. 2018, doi: 10.1109/TIA.2018.2829468.

[96] B. Zhao, Q. Song, W. Liu, and Y. Sun, "Overview of dual-active-bridge isolated bidirectional DC–DC converter for high-frequency-link power-conversion system," *IEEE Trans. Power Electron.*, vol. 29, no. 8, pp. 4091–4106, Aug. 2014, doi: 10.1109/TPEL.2013.2289913.

[97] N. Hou and Y. W. Li, "Overview and comparison of modulation and control strategies for a nonresonant single-phase dual-active-bridge DC–DC converter," *IEEE Trans. Power Electron.*, vol. 35, no. 3, pp. 3148–3172, Mar. 2020, doi: 10.1109/TPEL.2019.2927930.

[98] S. Shao, H. Chen, X. Wu, J. Zhang, and K. Sheng, "Circulating current and ZVS-on of a dual active bridge DC-DC converter: A review," *IEEE Access*, vol. 7, pp. 50561–50572, 2019, doi: 10.1109/ACCESS.2019.2911009.

[99] W. Zhao, X. Zhang, S. Gao, and M. Ma, "Improved model-based phase-shift control for fast dynamic response of dual-active-bridge DC/DC converters," *IEEE J. Emerg. Sel. Topics Power Electron.*, vol. 9, no. 1, pp. 223–231, Feb. 2021, doi: 10.1109/JESTPE.2020.2972960.

[100] H. Bai and C. Mi, "Eliminate reactive power and increase system efficiency of isolated bidirectional dual-active-bridge DC–DC converters using novel dual-phase-shift control," *IEEE Trans. Power Electron.*, vol. 23, no. 6, pp. 2905–2914, Nov. 2008, doi: 10.1109/TPEL.2008.2005103.

[101] B. Zhao, Q. Song, and W. Liu, "Efficiency characterization and optimization of isolated bidirectional DC–DC converter based on dual-phase-shift control for DC distribution application," *IEEE Trans. Power Electron.*, vol. 28, no. 4, pp. 1711–1727, Apr. 2013, doi: 10.1109/TPEL.2012.2210563.

[102] S. S. Muthuraj, V. K. Kanakesh, P. Das, and S. K. Panda, "Triple phase shift control of an LLL tank based bidirectional dual active bridge converter," *IEEE Trans. Power Electron.*, vol. 32, no. 10, pp. 8035–8053, Oct. 2017, doi: 10.1109/TPEL.2016.2637506.

[103] J. Huang, Y. Wang, Z. Li, and W. Lei, "Unified triple-phase-shift control to minimize current stress and achieve full soft-switching of isolated bidirectional DC–DC converter," *IEEE Trans. Ind. Electron.*, vol. 63, no. 7, pp. 4169–4179, Jul. 2016, doi: 10.1109/TIE.2016.2543182.

[104] G. G. Oggier, R. Leidhold, G. O. Garcia, A. R. Oliva, J. C. Balda, and F. Barlow, "Extending the ZVS operating range of dual active bridge high-power DC-DC converters," in *Proc. 37th IEEE Power Electron. Specialists Conf.*, 2006, pp. 1–7, doi: 10.1109/pesc.2006.1712142.

[105] G. G. Oggier, G. O. GarcÍa, and A. R. Oliva, "Switching control strategy to minimize dual active bridge converter losses," *IEEE Trans. Power Electron.*, vol. 24, no. 7, pp. 1826–1838, Jul. 2009, doi: 10.1109/TPEL.2009.2020902.

[106] M. Mahdavifard, N. Mazloum, F. Zahin, A. KhakparvarYazdi, A. Abasian, and S. A. Khajehoddin, "An asymmetrical DAB converter modulation and control systems to extend the ZVS range and improve efficiency," *IEEE Trans. Power Electron.,* vol. 37, no. 10, pp. 12774–12792, Oct. 2022, doi: 10.1109/TPEL.2022.3177401.

[107] W. Choi, K. Rho, and B. Cho, "Fundamental duty modulation of dual-active-bridge converter for wide-range operation," *IEEE Trans. Power Electron.*, vol. 31, no. 6, pp. 4048–4064, Jun. 2016, doi: 10.1109/TPEL.2015.2474135.

[108] T. Saha, A. C. Bagchi, and R. A. Zane, "Analysis and design of an LCL–T resonant DC–DC converter for underwater power supply," *IEEE Trans. Power Electron.*, vol. 36, no. 6, pp. 6725–6737, Jun. 2021, doi: 10.1109/TPEL.2020.3034298.

[109] J. Huang et al., "Robust circuit parameters design for the CLLC-Type DC transformer in the hybrid AC–DC microgrid," *IEEE Trans. Ind. Electron.*, vol. 66, no. 3, pp. 1906–1918, Mar. 2019, doi: 10.1109/TIE.2018.2835373.

[110] M. Yaqoob, K. H. Loo, and Y. M. Lai, "A Four-Degrees-of-Freedom modulation strategy for dual-active-bridge series-resonant converter designed for total loss minimization," *IEEE Trans. Power Electron.*, vol. 34, no. 2, pp. 1065–1081, Feb. 2019, doi: 10.1109/TPEL.2018.2865969.

[111] S. S. Shah, S. K. Rastogi, and S. Bhattacharya, "Paralleling of LLC resonant converters," *IEEE Trans. Power Electron.*, vol. 36, no. 6, pp. 6276–6287, Jun. 2021, doi: 10.1109/TPEL.2020.3040621.

[112] T. Duman, S. Marti, M. A. Moonem, A. A. R. Abdul Kader, and H. Krishnaswami, "A modular multilevel converter with power mismatch control for grid-connected photovoltaic systems," *Energies*, vol. 10, no. 698, pp. 1–28, May 2017, doi: 10.3390/en10050698.

[113] L. H. Meneghetti et al., "Hybrid inverter and control strategy for enabling the PV generation dispatch using extra-low-voltage batteries," *Energies*, vol. 15, no. 20, pp. 1–20, Oct. 2022, doi: 10.3390/en15207539.

[114] L. H. Meneghetti et al., "Multifunctional PV converter for uninterrupted power supply," in *Proc. IEEE PES Innov. Smart Grid Technol. Conf.-Latin Amer.*, 2019, pp. 1–6, doi: 10.1109/ISGT-LA.2019.8895322.

[115] L. H. Meneghetti et al., "Control strategy and power management for multifunctional inverters with BESS and reactive power compensation," in *Proc. IEEE 15th Braz. Power Electron. Conf. 5th IEEE Southern Power Electron. Conf.*, 2019, pp. 1–6, doi: 10.1109/COBEP/SPEC44138.2019.9065726.

[116] W.-S. Lee, J.-H. Kim, J.-Y. Lee, and I.-O. Lee, "Design of an isolated DC/DC topology with high efficiency of over 97% for EV fast chargers," *IEEE Trans. Veh. Technol.*, vol. 68, no. 12, pp. 11725–11737, Dec. 2019, doi: 10.1109/TVT.2019.2949080.

[117] P. He and A. Khaligh, "Comprehensive analyses and comparison of 1 kW isolated DC–DC converters for bidirectional EV charging systems," *IEEE Trans. Transp. Electrific.*, vol. 3, no. 1, pp. 147–156, Mar. 2017, doi: 10.1109/TTE.2016.2630927.

[118] E. L. Carvalho, L. H. Meneghetti, L. Bellinaso, R. Cardoso, and L. Michels, "Bidirectional interlink converter for bipolar DC microgrids," in *Proc. IEEE PES Innov. Smart Grid Technol. Conf.*, 2019, pp. 1–6, doi: 10.1109/ISGT-LA.2019.8895334.

[119] E. L. Carvalho, L. V. Bellinaso, R. Cardoso, and L. Michels, "Price-Based DC bus signaling for nanogrids power management," in *Proc. Braz. Power Electron. Conf.*, 2021, pp. 1–5, doi: 10.1109/COBEP53665.2021.9684069.

[120] E. L. Carvalho, L. V. Bellinaso, R. Cardoso, and L. Michels, "Experimental evaluation of a dual DC buses nanogrid with interlink converter," in *Proc. Braz. Power Electron. Conf.*, 2021, pp. 1–5, doi: 10.1109/COBEP53665.2021.9684037.

[121] E. L. Carvalho, A. Blinov, A. Chub, and D. Vinnikov, "Analysis of holdup time for DC grid-forming isolated active front-end converters," in *Proc. 48th Annu. Conf. Ind. Electron. Soc.*, 2022, pp. 1–6.

[122] L. Gu and S. Chang, "A nine-bridge single-stage isolated three-phase bidirectional AC/DC converter," in *Proc. 46th Annu. Conf. IEEE Ind. Electron. Soc.*, 2020, pp. 4147–4151, doi: 10.1109/IECON43393.2020.9254536.

[123] R. Huang and S. K. Mazumder, "A soft-switching scheme for an isolated DC/DC converter with pulsating DC output for a three-phase high-frequency-link PWM converter," *IEEE Trans. Power Electron.*, vol. 24, no. 10, pp. 2276–2288, Oct. 2009, doi: 10.1109/TPEL.2009.2022755.

[124] S. Zengin and M. Boztepe, "A novel current modulation method to eliminate low-frequency harmonics in single-stage dual active bridge AC–DC converter," *IEEE Trans. Ind. Electron.*, vol. 67, no. 2, pp. 1048–1058, Feb. 2020, doi: 10.1109/TIE.2019.2898597.

[125] T. Chen, R. Yu, and A. Q. Huang, "Variable-Switching-Frequency single-stage bidirectional GaN AC–DC converter for the grid-tied battery energy storage system," *IEEE Trans. Ind. Electron.*, vol. 69, no. 11, pp. 10776–10786, Nov. 2022, doi: 10.1109/TIE.2021.3120483.

[126] M. Silva, N. Hensgens, J. A. Oliver, P. Alou, Ó. García, and J. A. Cobos, "Isolated swiss-forward three-phase rectifier with resonant reset," *IEEE Trans. Power Electron.*, vol. 31, no. 7, pp. 4795–4808, Jul. 2016, doi: 10.1109/TPEL.2015.2482600.

[127] B. Zhang, S. Xie, Z. Li, P. Zhao, and J. Xu, "An optimized single-stage isolated swiss-type AC/DC converter based on single full-bridge with midpoint-clamper," *IEEE Trans. Power Electron.*, vol. 36, no. 10, pp. 11288–11297, Oct. 2021, doi: 10.1109/TPEL.2021.3073742.

[128] B. Zhang, S. Xie, J. Xu, K. Xu, and Z. Li, "An optimized single-stage isolated phase-shifted full-bridge based Swiss-rectifier," in *Proc. 45th Annu. Conf. IEEE Ind. Electron. Soc.*, 2019, pp. 6581–6586, doi: 10.1109/IECON.2019.8926934.

[129] J.-S. Lee and K.-B. Lee, "An open-switch fault detection method and tolerance controls based on SVM in a grid-connected T-Type rectifier with unity power factor," *IEEE Trans. Ind. Electron.*, vol. 61, no. 12, pp. 7092–7104, Dec. 2014, doi: 10.1109/TIE.2014.2316228.

[130] J. Lee, U. Choi, and K. Lee, "Comparison of tolerance controls for open-switch fault in a grid-connected T-Type rectifier," *IEEE Trans. Power Electron.*, vol. 30, no. 10, pp. 5810–5820, Oct. 2015, doi: 10.1109/TPEL.2014.2369414.

[131] Y. Li, J. Schäfer, D. Bortis, J. W. Kolar, and G. Deboy, "Optimal synergetic control of a three-phase two-stage ultra-wide output voltage range EV battery charger employing a novel hybrid quantum series resonant DC/DC converter," in *Proc. IEEE 21st Workshop Control Model. Power Electron.*, 2020, pp. 1–11, doi: 10.1109/COMPEL49091.2020.9265732.

[132] D. Zhang, M. Guacci, M. Haider, D. Bortis, J. W. Kolar, and J. Everts, "Three-Phase bidirectional buck-boost current DC-Link EV battery charger featuring a wide output voltage range of 200 to 1000V," in *Proc. IEEE Energy Convers. Congr. Expo.*, 2020, pp. 4555–4562, doi: 10.1109/ECCE44975.2020.9235868.

[133] Y. Li, J. A. Anderson, J. Schäfer, D. Bortis, J. W. Kolar, and J. Everts, "Control and protection of a synergetically controlled two-stage boost-buck PFC rectifier system under irregular grid conditions," in *Proc. IEEE 9th Int. Power Electron. Motion Control Conf.*, 2020, pp. 422–429, doi: 10.1109/IPEMC-ECCEAsia48364.2020.9367872.

[134] J. A. Anderson, M. Haider, D. Bortis, J. W. Kolar, M. Kasper, and G. Deboy, "New synergetic control of a 20kW isolated VIENNA rectifier front-end EV battery charger," in *Proc. 20th Workshop Control Model. Power Electron.*, 2019, pp. 1–8, doi: 10.1109/COMPEL.2019.8769657.

[135] A. Blinov, D. Zinchenko, J. Rąbkowski, G. Wrona, and D. Vinnikov, "Quasi single-stage three-phase filterless converter for EV charging applications," *IEEE Open J. Power Electron.*, vol. 3, pp. 51–60, 2022, doi: 10.1109/OJPEL.2021.3134460.

[136] W. W. Chen, R. Zane, and L. Corradini, "Isolated bidirectional grid-tied three-phase AC–DC power conversion using series-resonant converter modules and a three-phase unfolder," *IEEE Trans. Power Electron.*, vol. 32, no. 12, pp. 9001–9012, Dec. 2017, doi: 10.1109/TPEL.2017.2652477.

[137] U. R. Prasanna and A. K. Rathore, "Analysis, design, and experimental results of a novel soft-switching snubberless current-fed half-bridge front-end converter-based PV inverter," *IEEE Trans. Power Electron.*, vol. 28, no. 7, pp. 3219–3230, Jul. 2013, doi: 10.1109/TPEL.2012.2222932.

[138] J. Afsharian, D. Xu, B. Wu, B. Gong, and Z. Yang, "The optimal PWM modulation and commutation scheme for a three-phase isolated buck matrix-type rectifier," *IEEE Trans. Power Electron.*, vol. 33, no. 1, pp. 110–124, Jan. 2018, doi: 10.1109/TPEL.2017.2661242.

[139] A. Blinov, D. Vinnikov, E. Romero-Cadaval, J. Martins, and D. Peftitsis, "Isolated high-frequency link PFC rectifier with high step-down factor and reduced energy circulation," *IEEE J. Emerg. Sel. Topics Ind. Electron.*, vol. 3, no. 3, pp. 788–796, Jul. 2022, doi: 10.1109/JESTIE.2021.3126226.

[140] A. Blinov, I. Verbytskyi, D. Peftitsis, and D. Vinnikov, "Regenerative passive snubber circuit for high-frequency link converters," *IEEE J. Emerg. Sel. Topics Ind. Electron.*, vol. 3, no. 2, pp. 252–257, Apr. 2022, doi: 10.1109/JESTIE.2021.3066897.

[141] A. Blinov et al., "High gain DC–AC high-frequency link inverter with improved quasi-resonant modulation," *IEEE Trans. Ind. Electron.*, vol. 69, no. 2, pp. 1465–1476, Feb. 2022, doi: 10.1109/TIE.2021.3060657.

[142] D. Zinchenko, A. Blinov, A. Chub, D. Vinnikov, I. Verbytskyi, and S. Bayhan, "High-Efficiency single-stage on-board charger for electrical vehicles," *IEEE Trans. Veh. Technol.*, vol. 70, no. 12, pp. 12581–12592, Dec. 2021, doi: 10.1109/TVT.2021.3118392.

[143] X. Yu, F. Jin, and M. Wang, "A novel soft-switching modulation scheme for isolated DC-to-three-phase-AC matrix-based converter using SiC device," in *Proc. IEEE Energy Convers. Congr. Expo.*, 2016, pp. 1–8, doi: 10.1109/ECCE.2016.7854746.

[144] J. Lu et al., "A modular-designed three-phase high-efficiency high-power-density EV battery charger using dual/triple-phase-shift control," *IEEE Trans. Power Electron.*, vol. 33, no. 9, pp. 8091–8100, Sep. 2018, doi: 10.1109/TPEL.2017.2769661.

[145] D. Sha, D. Zhang, and J. Zhang, "A single-stage dual-active-bridge AC–DC converter employing mode transition based on real-time calculation," *IEEE Trans. Power Electron.*, vol. 36, no. 9, pp. 10081–10088, Sep. 2021, doi: 10.1109/TPEL.2021.3058143.

[146] A. K. Bhattacharjee and I. Batarseh, "An interleaved boost and dual active bridge-based single-stage three-port DC–DC–AC converter with sine PWM modulation," *IEEE Trans. Ind. Electron.*, vol. 68, no. 6, pp. 4790–4800, Jun. 2021, doi: 10.1109/TIE.2020.2992956.

[147] J. Saha, N. B. Y. Gorla, and S. K. Panda, "Implementation of power balance control scheme for a cascaded matrix-based dual-active-bridge (CMB-DAB) MVAC–LVDC converter," *IEEE Transaction Ind. Appl.*, vol. 58, no. 1, pp. 388–399, Feb. 2022, doi: 10.1109/TIA.2021.3118657.

[148] N. D. Dao and D.-C. Lee, "Modulation and control of single-stage bidirectional isolated direct-matrix-based AC-DC converters," in *Proc. 10th Int. Conf. Power Electron. ECCE Asia*, 2019, pp. 2278–2283, doi: 10.23919/ICPE2019-ECCEAsia42246.2019.8797356.

[149] A. Shawky, T. Takeshita, and M. A. Sayed, "Single-Stage three-phase grid-tied isolated SEPIC-Based differential inverter with improved control and selective harmonic compensation," *IEEE Access*, vol. 8, pp. 147407–147421, 2020, doi: 10.1109/ACCESS.2020.3014894.

[150] A. Shawky, T. Takeshita, M. A. Sayed, M. Aly, and E. M. Ahmed, "Improved controller and design method for grid-connected three-phase differential SEPIC inverter," *IEEE Access*, vol. 9, pp. 58689–58705, 2021, doi: 10.1109/ACCESS.2021.3072489.

[151] H. -S. Kim, J.-W. Baek, M.-H. Ryu, J.-H. Kim, and J.-H. Jung, "The high-efficiency isolated AC–DC converter using the three-phase interleaved LLC resonant converter employing the Y-Connected rectifier," *IEEE Trans. Power Electron.*, vol. 29, no. 8, pp. 4017–4028, Aug. 2014, doi: 10.1109/TPEL.2013.2290999.

[152] D. Sal y Rosas, "Isolated and bidirectional Three-phase AC-DC converter composed of three unfolding bridges cascaded with a quad-active-bridge series-resonant DC-DC converter," in *Proc. 23rd Eur. Conf. Power Electron. Appl.*, 2021, pp. 1–7.

[153] B. J. D. Vermulst, J. L. Duarte, C. G. E. Wijnands, and E. A. Lomonova, "Quad-Active-Bridge single-stage bidirectional three-phase AC–DC converter with isolation: Introduction and optimized modulation," *IEEE Trans. Power Electron.*, vol. 32, no. 4, pp. 2546–2557, Apr. 2017, doi: 10.1109/TPEL.2016.2579682.

[154] S. S. Queiroz, D. S. Oliveira, P. P. Praça, L. Henrique, and S. C. Barreto, "Interleaving technique applied in an active filter based on the full-bridge cascaded converter," in *Proc. IEEE Appl. Power Electron. Conf. Expo.*, 2020, pp. 2313–2318, doi: 10.1109/APEC39645.2020.9124453.

[155] D. S. Oliveira and B. R. D. Almeida, "A bidirectional Single-stage three-phase AC/DC converter with high-frequency isolation and PFC," in *Proc. PCIM Europe 2015; Int. Exhib. Conf. Power Electron., Intell. Motion, Renewable Energy Energy Manage.*, 2015, pp. 1–8.

[156] J. W. M. Araújo, D. S. O. Júnior, P. P. Praça, L. H. S. C. Barreto, D. de A. Honório, and F. L. M. Antunes, "Experimental validation of a basic module based on a single-stage AC-DC converter, feasible to solid-state transformer applications," in *Proc. 21st Eur. Conf. Power Electron. Appl.*, 2019, pp. 1–7, doi: 10.23919/EPE.2019.8914989.

[157] B. R. de Almeida, D. de Souza Oliveira, and P. P. Praça, "A bidirectional single-stage three-phase rectifier with high-frequency isolation and power factor correction," in *Proc. IEEE Appl. Power Electron. Conf. Expo.*, 2016, pp. 60–65, doi: 10.1109/APEC.2016.7467852.

[158] D. S. Oliveira, D. d. A. Honorio, L. H. S. C. Barreto, and P. P. Praca, "A single-stage AC-DC modular cascaded multilevel converter feasible to SST applications," in *Proc. PCIM Europe 2015; Int. Exhib. Conf. Power Electron., Intell. Motion, Renewable Energy Energy Manage.*, 2015, pp. 1–8.

[159] D. d. A. Honório, D. S. Oliveira, L. H. S. C. Barreto, and F. L. M. Antunes, "A solid state transformer based on a single-stage AC-DC modular cascaded multilevel converter," in *Proc. 18th Eur. Conf. Power Electron. Appl.*, 2016, pp. 1–9, doi: 10.1109/EPE.2016.7695375.

[160] H. A. De Oliveira, B. C. Torrico, D. De S. Oliveira, S. G. Barbosa, and M. P. De Almeida Filho, "Predictive control applied to a single-stage, single-phase bidirectional AC-DC converter," *IEEE Access*, vol. 10, pp. 34984–34995, 2022, doi: 10.1109/ACCESS.2022.3161524.
[161] H. Fathabadi, "Novel wind powered electric vehicle charging station with vehicle-to-grid (V2G) connection capability," *Energy Convers. Manage.*, vol. 136, pp. 229–239, 2017, doi: 10.1016/j.enconman.2016.12.045.
[162] A. Singh, A. K. Yadav, and A. Khaligh, "Steady-State modeling of a dual-active bridge AC–DC converter considering circuit nonidealities and intracycle transient effects," *IEEE Trans. Power Electron.*, vol. 36, no. 10, pp. 11276–11287, Oct. 2021, doi: 10.1109/TPEL.2021.3073350.
[163] S. Luo, F. Wu, and G. Wang, "Single-Stage hybrid three-level DAB type resonant AC–DC converter," *IEEE Trans. Transp. Electrific.*, vol. 8, no. 1, pp. 799–807, Mar. 2022, doi: 10.1109/TTE.2021.3101618.
[164] P. Emiliani, A. Blinov, A. Chub, and D. Vinnikov, "DC grid interface converter based on Three-phase isolated matrix topology with phase-shift modulation," in *Proc. IEEE 13th Int. Symp. Power Electron. Distrib. Gener. Syst.*, 2022, pp. 1–7.
[165] F. Flores-Bahamonde, H. Renaudineau, A. M. Llor, A. Chub, and S. Kouro, "The DC transformer power electronic building block: Powering next-generation converter design," *IEEE Ind. Electron. Mag.*, early access, Feb. 21, 2022, doi: 10.1109/MIE.2022.3147168.
[166] U. Nasir, A. Costabeber, P. Wheeler, M. Rivera, and J. Clare, "A three-phase modular isolated matrix converter," *IEEE Trans. Power Electron.*, vol. 34, no. 12, pp. 11760–11773, Dec. 2019, doi: 10.1109/TPEL.2019.2909681.
[167] J. E. Huber, J. Böhler, D. Rothmund, and J. W. Kolar, "Analysis and cell-level experimental verification of a 25 kW all-SiC isolated front end 6.6 kV/400 V AC-DC solid-state transformer," *CPSS Trans. Power Electron. Appl.*, vol. 2, no. 2, pp. 140–148, 2017, doi: 10.24295/CPSSTPEA.2017.00014.
[168] M. A. Awal et al., "Capacitor voltage balancing for neutral point clamped dual active bridge converters," *IEEE Trans. Power Electron.*, vol. 35, no. 10, pp. 11267–11276, Oct. 2020, doi: 10.1109/TPEL.2020.2988272.
[169] P. Liu, C. Chen, S. Duan, and W. Zhu, "Dual phase-shifted modulation strategy for the three-level dual active bridge DC–DC converter," *IEEE Trans. Ind. Electron.*, vol. 64, no. 10, pp. 7819–7830, Oct. 2017, doi: 10.1109/TIE.2017.2696488.

EDIVAN LAERCIO CARVALHO (Member, IEEE) received the B.Sc. and M.Sc. degrees in electrical engineering from the Federal University of Technology – Paraná, Pato Branco, Brazil, in 2015, and 2018, respectively, and the Ph.D. degree in electrical engineering from the Federal University of Santa Maria, Santa Maria, Brazil. He spent one year as an R&D Engineer with WEG Drives and Controls in 2021, Jaraguá do Sul, Brazil. He is currently a Postdoctoral Researcher with the Tallinn University of Technology, Tallin, Estonia. His research interests include high-frequency power converter topologies, net-zero energy buildings, nanogrids, and power management systems.

ANDREI BLINOV (Senior Member, IEEE) received the M.Sc. degree in electrical drives and power electronics and the Ph.D. degree, with a dissertation devoted to the research of switching properties and performance improvement methods of high-voltage IGBT-based dc–dc converters, from the Tallinn University of Technology, Tallinn, Estonia, in 2008 and 2012, respectively. After the Ph.D. degree, he spent two years in Sweden a Postdoctoral Researcher with the KTH Royal Institute of Technology, Stockholm, Sweden. He is currently a Senior Researcher with the Department of Electrical Power Engineering and Mechatronics, Tallinn University of Technology. His research interests include the research of switch-mode power converters, new semiconductor technologies, and energy storage systems.

ANDRII CHUB (Senior Member, IEEE) received the B.Sc. and M.Sc. degrees in electronic systems from Chernihiv State Technological University, Chernihiv, Ukraine, in 2008 and 2009, respectively, and the Ph.D. degree in electrical engineering from the Tallinn University of Technology, Tallinn, Estonia, in 2016. He was with Kiel University, Kiel, Germany, in 2017 and Federico Santa Maria Technical University, Valparaíso, Chile, from 2018 to 2019. He is currently a Senior Researcher with the Power Electronics Group, Tallinn University of Technology. He has coauthored more than 100 articles on power electronics and applications. His research interests include advanced dc–dc converter topologies, renewable energy conversion systems, energy-efficient buildings, reliability, and fault-tolerance of power electronic converters.

PIETRO EMILIANI (Student Member, IEEE) received the B.Sc. and M.Sc. degrees (*cum laude*) in electrical engineering from the Politecnico di Milano, Milan, Italy, in 2021. He is currently working toward the Ph.D. degree with the Power Electronics Group, Tallinn University of Technology, Tallinn, Estonia. His research interests include power electronics and dc distribution grids, with a focus on energy management systems for residential microgrids with integrated energy storage.

GIOVANNI DE CARNE (Senior Member, IEEE) received the B.Sc. and M.Sc. degrees in electrical engineering from the Polytechnic University of Bari, Bari, Italy, in 2011 and 2013, respectively, and the Ph.D. degree in electrical engineering from the Chair of Power Electronics, Kiel University, Kiel, Germany, in 2018. Till 2019, he was a Postdoctoral Fellow with Kiel University working on HVdc control and services. He is currently the Head of the Real Time System Integration Group and Power Hardware In the Loop Lab, Institute for Technical Physics, Karlsruhe Institute of Technology, Karlsruhe, Germany. He has authored or coauthored more than 60 peer-reviewed scientific papers. His research interests include power electronics transformers, real time modeling, and power hardware in the loop. Dr. De Carne was the recipient of the Helmholtz Young Investigator Group for the project Hybrid networks: a multi-modal design for the future energy system in 2020. He is also the Chairman of the IEEE PES Task Force on Solid state transformer integration in distribution grids, and an Associate Editor for *IEEE Industrial Electronics Magazine* and IEEE Open Journal of Power Electronics.

DMITRI VINNIKOV (Senior Member, IEEE) received the Dipl.Eng., M.Sc., and Dr.Sc.techn. degrees in electrical engineering from the Tallinn University of Technology, Tallinn, Estonia, in 1999, 2001, and 2005, respectively. He is currently the Head of the Power Electronics Group, Department of Electrical Power Engineering and Mechatronics, Tallinn University of Technology. Moreover, he is one of the founders and leading researchers of ZEBE—Estonian Centre of Excellence for zero energy and resource efficient smart buildings and districts. He has authored or coauthored two books, five monographs, and one book chapter and more than 400 published articles on power converter design and development and is the holder of numerous patents and utility models in this field. His research interests include applied design of power electronic converters and control systems, renewable energy conversion systems (photovoltaic and wind), impedance-source power converters, and implementation of wide bandgap power semiconductors. He is the Chair of the IEEE Estonia Section.